Ultrasound
in medicine
and biology

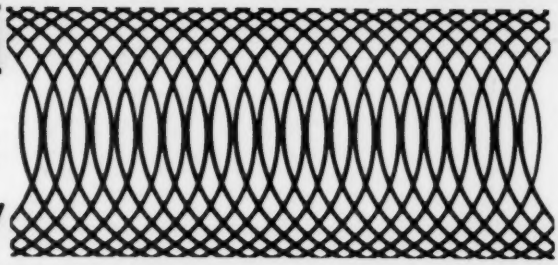

Supplement to *Ultrasound in Medicine and Biology*, Volume 22, Number 4, 1996

Author–Subject Index
Volume 21 (1995)

Compiled by

Michael Halliwell
Department of Medical Physics, Bristol General Hospital, Bristol BS1 6SY, United Kingdom

ELSEVIER

ULTRASOUND IN MEDICINE AND BIOLOGY

WORLD FEDERATION FOR ULTRASOUND IN MEDICINE AND BIOLOGY

President: B. B. GOLDBERG, *USA*

Past-President: M. FUKUDA, *Japan*

President-Elect: H. LUTZ, *Germany*

Vice-President I: H. WATANABE, *Japan*

Vice-President II: D. E. ROBINSON, *Australia*

Treasurer: M. C. ZISKIN, *USA*

Secretary: S. HANCKE, *Denmark*

Administrative Councillors:

G. G. CERRI, *Brazil*

H. Y. CHEN, *Taiwan*

S. EIK-NES, *Norway*

C. R. B. MERRITT, *USA*

Co-opted Councillors:

C. A. BRUGUERA, *Argentina*

H. GHARBI, *Tunisia*

M. MAKUUCHI, *Japan*

Editor-in-Chief:

P. N. T. WELLS, *UK*

AFFILIATED SOCIETIES

American Institute of Ultrasound in Medicine (AIUM), A. B. Kurtz, Secretary, 14750 Sweitzer Lane, Suite 100, Laurel, MD 20707, USA

Asian Federation of Societies for Ultrasound in Medicine and Biology (AFSUMB), K. Nakayama, Secretary, Faculty of Science and Technology, Sophia University, 7-1 Kioicho, Chiyoda-ku, Tokyo, Japan

Australasian Society for Ultrasound in Medicine (ASUM), S. Butterworth, Executive Secretary, 2/181 High Street, Willoughby, NSW 2068, Australia

European Federation of Societies for Ultrasound in Medicine and Biology (EFSUMB), E. Brown, General Secretary, 36 Portland Place, London W1N 3DG, UK

Latin-American Federation of Societies for Ultrasound in Medicine and Biology (FLAUS), G. G. Cerri, Permanent Secretary, Av. Paulista, 491 13° conj. 132, CEP 01311, São Paulo, Brazil

Mediterranean and African Society for Ultrasound (MASU), H. A. Gharbi, Secretary, 12 Ruc Mohamed Salahoddine, 1082 Tunis, Tunisia

Production Editor: A. Bakken, E-mail: A.BAKKEN@ELSEVIER.COM

Publishing and Advertising Office: Elsevier Science Inc., 660 White Plains Road, Tarrytown, NY 10591-5153, USA, E-mail Address: ESUK.USA@ELSEVIER.COM.

Please direct inquiries regarding advertising in this journal to Jay Allan Feinman, Advertising Sales Dept., Elsevier Science Inc., 660 White Plains Road, Tarrytown, NY 10591-5153. Tel: (914) 333-2457, Fax: (914) 333-2444, E-Mail: j.feinman@elsevier.com.

Reprints of any article in this journal are available for purchase in quantities of 100 or more. Please contact Kristin Couch, Commercial Reprints Dept., Elsevier Science Inc., 660 White Plains Road, Tarrytown, NY 10591-5153. Tel: (914) 333-2555, Fax: (914) 333-2444, E-Mail: k.couch@elsevier.com.

Subscription Office: Elsevier Science Inc., 655 Avenue of the Americas, New York, NY 10010-5107, USA. For customer service: phone (212) 633-3950 or fax (212) 633-3990.

Published 9 per Annum. *Annual Institutional Subscription Rate* (1996): US$685.00. Price includes postage and insurance and is subject to change without notice. Members of the World Federation for Ultrasound in Medicine and Biology may order personal subscriptions at a concessional rate; details of these rates are available upon request.

ELSEVIER

Ultrasound in Med. & Biol., Vol. 22, Suppl., pp. 1–76, 1996
Copyright © 1996 World Federation for Ultrasound in Medicine & Biology
Printed in the USA. All rights reserved
0301-5629/96 $15.00 + .00

AUTHOR/SUBJECT INDEX

A

Aarnink, R. G. and Wijkstra, H.: errors in transrectal ultrasonic planimetry of the prostate: computer simulation of volumetric errors applied to a screening population: regarding Bangma et al. UMB 21(1):11–16; 1995, 1083

Abdominal circumference
scapula length measurement for assessment of fetal growth and development (Dilmen), 139

Ablation
modification of intensity distributions from large aperture ultrasound sources (Clarke), 353
physical factors involved in stress-wave-induced cell injury: the effect of stress gradient (Doukas), 961

Absorption spectroscopy
damage to red blood cells induced by acoustic cavitation (Daniels), 105

Achaibou, F., see Arbeille, Ph.

Acoustic energy (see also ESWL)
acoustic energy determines haemoglobin release from erythrocytes by extracorporeal shock waves *in vitro* (Delius), 707

Acoustic exposure
a theory to correct the systematic error caused by the imperfectly matched beam width to vessel diameter ratio on volumetric flow measurements using ultrasound techniques (Fei), 1047

Acoustic impedance
echogenicity of experimental liver ethanol injections (Vehmas), 1137

Acoustic output
a theory to correct the systematic error caused by the imperfectly matched beam width to vessel diameter ratio on volumetric flow measurements using ultrasound techniques (Fei), 1047
how reliable are manufacturer's reported acoustic output data? (Jago), 135
the performance of different pressure pulse generators for extracorporeal lithotripsy: a comparison based on commercial lithotripters for kidney stones (Buizza), 259

Acoustic properties
acoustic properties of some biocompatible polymers at body temperature (Guess), 273

Acoustic scatterer
preliminary investigation of ultrasound scattering analysis to identify women at risk for later invasive cancer. I: motivation and experimental technique for characterization of isolated breast tissue lobules (Burke), 295
preliminary investigation of ultrasound scattering analysis to identify women at risk for later invasive cancer. II: extraction of dominant scattering angle-dependent trends from excised breast tissue (Burke), 305

Acute pelvic inflammatory disease
the value of transvaginal color Doppler in the assessment of pelvic inflammatory disease (Kupesic), 733

Adams, D. B., see Smith, S. W.
Adams, T., see Coleman, A. J.
Adler, R. S., see Chen, E. J.
Adler, R. S., Rubin, J. M., Fowlkes, J. B., Carson, P. L. and Pallister, J. E.: ultrasonic estimation of tissue perfusion: a stochastic approach, 493

Adnexal masses
serial assessment of adnexal masses with transvaginal color Doppler sonography (Fleischer), 435

Adult testis
the effect of ultrasound exposure *in utero* on the development of the fetal mouse testis: adult consequences (Carnes), 1247

Al Diek, Y., see Delius, M.
Alam, S. K. and Parker, K. J.: the butterfly search technique for estimation of blood velocity, 657

Albunex
time-domain ultrasonic contrast blood flowmetry (Shung), 71

Aliasing
transesophageal color Doppler evaluation of obstructive lesions using the new "Quasar" technology (Fan), 1021

Allard, L., Cloutier, G. and Durand, L.-G.: Doppler velocity ratio measurements evaluated in a phantom model of multiple arterial disease, 471
Allard, L., see Cloutier, G.
Aayiotos, A. S., Perry, G. J., Myers, J. G., Green, D. W., Fan, P. H. and Nanda, N. C.: a numerical and experimental investigation of the flow acceleration region proximal to an orifice, 501

Angle dependent scatter
preliminary investigation of ultrasound scattering analysis to identify women at risk for later invasive cancer. I: motivation and experimental technique for characterization of isolated breast tissue lobules (Burke), 295
preliminary investigation of ultrasound scattering analysis to identify women at risk for later invasive cancer. II: extraction of dominant scattering angle-dependent trends from excised breast tissue (Burke), 305

Angle independent flow
experimental velocity profiles and volumetric flow via two-dimensional speckle tracking (Bohs), 885

Animal model
quantification of intravenous contrast-enhanced Doppler power spectrum in the rabbit carotid artery (Frush), 41

Aorta compression
assessment of the fetal PO_2 changes by cerebral and umbilical Doppler on lamb fetuses during acute hypoxia (Arbeille), 861

Apodization
modification of intensity distributions from large aperture ultrasound sources (Clarke), 353

dell'Aquila, T., see Buizza, A.
Arbeille, P., Maulik, D., Fignon, A., Stale, H., Berson, M., Bodard, S. and Locatelli, A.: assessment of the fetal PO_2 changes by cerebral and umbilical Doppler on lamb fetuses during acute hypoxia, 861
Arbeille, Ph., Berson, M., Achaibou, F., Bodard, S. and Locataelli, A.: vascular resistance quantification in high flow resistance areas using the Doppler method, 321

Artefact suppression
blood perfusion measurement with multifrequency Doppler ultrasound (Eriksson), 49

Artefacts
blood perfusion measurement with multifrequency Doppler ultrasound (Eriksson), 49
transesophageal color Doppler evaluation of obstructive lesions using the new "Quasar" technology (Fan), 1021
velocity matched spectrum analysis: a new method for suppressing velocity ambiguity in pulsed-wave Doppler (Torp), 937

Arterial distensibility
assessment of regional vascular distensibility in diseased iliofemoral arteries by intravascular ultrasound (The), 17

Arterial occlusive disease
Doppler ultrasound spectral shape downstream of significant arterial stenosis *in vivo* (Hutchison), 447
Doppler velocity ratio measurements evaluated in a phantom model of multiple arterial disease (Allard), 471
effects of stenosis on transit-time ultrasound measurements of blood flow (Gordon), 623

Arterial stenosis
Doppler ultrasound spectral shape downstream of significant arterial stenosis *in vivo* (Hutchison), 447
Doppler velocity ratio measurements evaluated in a phantom model of multiple arterial disease (Allard), 471
effects of stenosis on transit-time ultrasound measurements of blood flow (Gordon), 623

Arterioles
effects of endothelin-1 on renal microvasculature measured using quantitative ultrasound (Insana), 1143

Artery
a noninvasive method to estimate wall shear rate using ultrasound (Brands), 171
assessment of regional vascular distensibility in diseased iliofemoral arteries by intravascular ultrasound (The), 17
changes in ultrasonic Doppler backscattered power downstream of concentric and eccentric stenoses under pulsatile flow (Cloutier), 59
computerised transient hyperaemic response test—a method for the assessment of cerebral autoregulation (Smielewski), 599
diameter and compliance in the human common carotid artery—variations with age and sex (Hansen), 1
discrimination of intravascular lumen and dissections in single intravascular ultrasound images using subtraction, conventional averaging and saline flush (Pasterkamp), 149
Doppler ultrasound spectral shape downstream of significant arterial stenosis *in vivo* (Hutchison), 447
Doppler velocity ratio measurements evaluated in a phantom model of multiple arterial disease (Allard), 471
effects of stenosis on transit-time ultrasound measurements of blood flow (Gordon), 623
intravascular ultrasound image subtraction: a contrast enhancing technique to facilitate automatic three-dimensional visualization of the arterial lumen (Pasterkamp), 913
is there a hemispheric side preference of cardiac valvular emboli? (Kaps), 753
quantification of intravenous contrast-enhanced Doppler power spectrum in the rabbit carotid artery (Frush), 41
reproducibility of Doppler measurements of blood flow velocity in the uterine and ovarian arteries in premenopausal women (Sladkevicius), 313
vascular resistance quantification in high flow resistance areas using the Doppler method (Arbeille), 321
velocity matched spectrum analysis: a new method for suppressing velocity ambiguity in pulsed-wave Doppler (Torp), 937
volumetric blood flow calculation using a narrow ultrasound beam (Willink), 203
volumetric blood flow measurement by simultaneous Doppler signal and B-mode image processing: a feasibility study (Willink), 481

Atherosclerosis
assessment of regional vascular distensibility in diseased iliofemoral arteries by intravascular ultrasound (The), 17
discrimination of intravascular lumen and dissections in single intravascular ultrasound images using subtraction, conventional averaging and saline flush (Pasterkamp), 149

Atrial fibrillation
quantification of blood echogenicity: evaluation of a semiquantitative method of grading spontaneous echo contrast (Fatkin), 1191

Atrial inflow
atrial inflow can alter regurgitant jet size: *in vitro* studies (Grimes), 459

Attenuation
acoustic properties of some biocompatible polymers at body temperature (Guess), 273

in situ human obstetrical ultrasound exposimetry: estimates of derating factors for each of three different tissue models (Siddiqi), 379
ultrasonic propagation properties of excised human skin (Moran), 1177

Augat, P. and Claes, L.: influence of water temperature on pressure pulses generated by an electromagnetic type lithotriper, 89

Autoregressive modeling
adaptive SVD-based AR model order determination for time-frequency analysis of Doppler ultrasound signals (Fort), 793

Autoregulation
computerised transient hyperaemic response test—a method for the assessment of cerebral autoregulation (Smielewski), 599

Azar, C., see Bastid, C.

B

B mode imaging
registration of three-dimensional compound ultrasound scans of the breast for refraction and motion correction (Moskalik), 769

B/A ratio
nonlinear behavior of a liquid containing uniform bubbles: comparison between theory and experiments (Wu), 545

Babcock, D. S., see Frush, D. P.

Background subtraction
background subtraction from time-intensity curves in videodensitometry: a pitfall in flow assessment using contrast echocardiography (Bos), 1211

Backscatter
a 40–100 MHz B-scan ultrasound backscatter microscope for skin imaging (Turnbull), 79
a survey of the acoustic outputs of diagnostic ultrasound equipment in current clinical use (Henderson), 699
changes in ultrasonic Doppler backscattered power downstream of concentric and eccentric stenoses under pulsatile flow (Cloutier), 59
characterization of ultrasonic B-scans using non-Rayleigh statistics (Molthen), 161
effects of endothelin-1 on renal microvasculature measured using quantitative ultrasound (Insana), 1143
preliminary investigation of ultrasound scattering analysis to identify women at risk for later invasive cancer. I: motivation and experimental technique for characterization of isolated breast tissue lobules (Burke), 295
preliminary investigation of ultrasound scattering analysis to identify women at risk for later invasive cancer. II: extraction of dominant scattering angle-dependent trends from excised breast tissue (Burke), 305
quantification of intravenous contrast-enhanced Doppler power spectrum in the rabbit carotid artery (Frush), 41
the subtleties of ultrasound images of an ensemble of cells: simulation from regular and more random distributions of scatterers (Hunt), 329
ultrasonic propagation properties of excised human skin (Moran), 1177
ultrasonic tissue characterization of end-stage dilated cardiomyopathy (Davison), 853

ultrasound backscatter at 30 MHz from human blood: influence of rouleau size affected by blood modification and shear rate (van der Heiden), 817
when can Doppler be used in place of integrated backscatter as a measure of scattered ultrasound intensity? (Schwarz), 231

Baert, L., see Pittomvils, G.

Balloon angioplasty
discrimination of intravascular lumen and dissections in single intravascular ultrasound images using subtraction, conventional averaging and saline flush (Pasterkamp), 149

Balls
ultrasound focal beam surgery (ter Haar), 1089

Bamber, J. C., see Bell, D. S.
Bamber, J. C., see Hirsch, W.
Bamber, J. C., see Moran, C.M.

Bandwidth
demonstration of three-dimensional vector flow estimation using bandwidth and two transducers on a flow phantom (McArdle), 679

Bangma, C. H., Hengeveld, E. J. and Schröder, F. H.: in response to Drs. Aarnink and Wijkstra, 1084
Bangma, C. H., Hengeveld, E. J., Niemer, A. Q. H. J. and Schröder, F. H.: errors in transrectal ultrasonic planimetry of the prostate: computer simulation of volumetric errors applied to a screening population, 11
Barnett, S. B., see Duggan, P. M.
Barr, L. L., see Frush, D. P.
Bastid, C., Azar, C. and Sahel, J.: ultrasound guided percutaneous ethanol treatment of hepatic neoplasms: a therapeutic alternative in the nineties, 129
Beach, K. W., see McArdle, A.

Beam characteristics
effects of non-uniform insonation by catheter-tipped Doppler transducers on velocity estimation (Moraes), 779

Beam cross section
blood perfusion measurement with multifrequency Doppler ultrasound (Eriksson), 49

Beam distortion
blood perfusion measurement with multifrequency Doppler ultrasound (Eriksson), 49

Beam distributions
modification of intensity distributions from large aperture ultrasound sources (Clarke), 353

Beam profile
acoustic energy determines haemoglobin release from erythrocytes by extracorporeal shock waves *in vitro* (Delius), 707
acoustic generation of intra-arterial contrast boluses (Ivey), 757
correction of intrinsic spectral broadening errors in Doppler peak velocity

measurements made with phased sector and linear array transducers (Winkler), 1029
effects of nonuniform insonation by catheter-tipped Doppler transducers on velocity estimation (Moraes), 779
influence of water temperature on pressure pulses generated by an electromagnetic type lithotripter (Augat), 89
modification of intensity distributions from large aperture ultrasound sources (Clarke), 353
ultrasonic heating of the brain of the fetal sheep *in utero* (Duggan), 553
ultrasound focal beam surgery (ter Haar), 1089

Beam steering
electronic beam steering of shock waves (Cathignol), 365

Beam tracking
feasibility study for a two-dimensional diagnostic ultrasound velocity mapping system (Phillips), 217

Beam width
a wall-less vessel phantom for Doppler ultrasound studies (Rickey), 1163

Becker, G., Krone, A., Schmitt, K., Woydt, M., Hofmann, E., Lindner, A., Bogdahn, U., Gahn, G. and Roosen, K.: preoperative and postoperative follow-up in high-grade gliomas: comparison of transcranial color-coded real-time sonography and computed tomography findings, 1123
Bell, D. S., Bamber, J. C. and Eckersley, R. J.: segmentation and analysis of colour Doppler images of tumour vasculature, 635
Bell, D. S., see Hirsch, W.
Benic, S., see Kupesic, S.

Benign prostatic hypertrophy (BPH)
reproducibility and observer variability of transrectal ultrasound measurements of prostatic volume (Collins), 1101
ultrasound and microbubbles: their generation, detection and potential utilization in tissue and organ therapy—experimental (Fry), 1227
ultrasound focal beam surgery (ter Haar), 1089

Berg, J., see Kaps, M.
Berson, M., see Arbeille, P.
Berson, M., see Arbeille, Ph.
Berstad, A., see Gilja, O. H.
Bezante, G. P., see Schwarz, K. Q.

Bias
bias in mean frequency estimation of Doppler signals due to wall clutter filters (Tysoe), 671
statistical bias and variance in blood flow estimation by spectral analysis of Doppler signals (Willink), 919

Bihrle, R., see Fry, F. J.

Biocompatible
acoustic properties of some biocompatible polymers at body temperature (Guess), 273

Bioeffects
a novel ultrasonic technique for differentiating cysts from solid lesions: preliminary results in the breast (Nightingale), 745
acoustic energy determines haemoglobin release from erythrocytes by extracorporeal shock waves *in vitro* (Delius), 707
acoustic generation of intra-arterial contrast boluses (Ivey), 757
biological effects of shock waves: *in vivo* effect of high energy pulses on rabbit bone (Delius), 1219
comet assay reveals DNA strand breaks induced by ultrasonic cavitation *in vitro* (Miller), 841
comparison of ultrasound irradiation of pregnant mice with other bioeffects data (Fry), 430
damage to red blood cells induced by acoustic cavitation (Daniels), 105
effect of therapeutic ultrasound on endochondral ossification (Wiltink), 121
effect of ultrasound on DNA synthesis in tumor cells (Forytková), 585
effects of piezoelectric lithotripsy on human DNA (Bird), 399
effects of ultrasound on agglutination and aggregation of human erythrocytes *in vitro* (Pohl), 711
flow cytometric analysis of cell suspensions exposed to shock waves in the presence of the radical sensitive dye Hydroethidine (Endl), 569
glycoprotein and ganglioside changes in human trophoblasts after exposure to pulsed Doppler ultrasound (Heffer-Lauc), 579
hematologic and growth-related effects of frequent prenatal ultrasound exposure in the long-tailed macaque (macaca fascicularis) (Tarantal), 1073
histologic effects of high intensity pulsed ultrasound exposure with subharmonic emission in rabbit brain *in vivo* (Vykhodtseva), 969
in situ human obstetrical ultrasound exposimetry: estimates of derating factors for each of three different tissue models (Siddiqi), 379
intestinal hemorrhage from exposure to pulsed ultrasound (Dalecki), 1067
microscopic lung alterations and reduction of respiration rate in insonated anesthetized swine (Harrison), 981
modification of intensity distributions from large aperture ultrasound sources (Clarke), 353
nonlinear behavior of a liquid containing uniform bubbles: comparison between theory and experiments (Wu), 545
physical factors involved in stress-wave-induced cell injury: the effect of stress gradient (Doukas), 961
pro- and antifibrinolytic effects of ultrasound on streptokinase-induced thrombolysis (Nilsson), 833
roles of hematocrit and fibrinogen in red cell aggregation determined by ultrasonic scattering properties (Kitamura), 827
the effect of ultrasound exposure *in utero* on the development of the fetal mouse testis: adult consequences (Carnes), 1247
the effects of successive high-energy shock-wave tumor administration on tumor blood flow (Cornel), 243
thresholds for hemorrhages in mouse skin and intestine induced by lithotripter shock waves (Miller), 249
ultrasonic heating of the brain of the fetal sheep *in utero* (Duggan), 553
ultrasound accelerates transport of recombinant tissue plasminogen activator into clots (Francis), 419
ultrasound and microbubbles: their generation, detection and potential utilization in tissue and organ therapy—experimental (Fry), 1227
venous thrombosis generation by means of high-intensity focused ultrasound (Delon-Martin), 113

Bird, N. C., Stephenson, T. J., Ross, B. and Johnson, A. G.: effects of piezoelectric lithotripsy on human DNA, 399
Birer, A., see Cathignol, D.
Blankenberg, F. G., see Burke, T. M.
Blankenberg, T. A., see Burke, T. M.
Blinc, A., see Francis, C. W.

Blood characterization
changes in ultrasonic Doppler backscattered power downstream of concentric and eccentric stenoses under pulsatile flow (Cloutier), 59

Blood echogenicity
ultrasound backscatter at 30 MHz from human blood: influence of rouleau size affected by blood modification and shear rate (van der Heiden), 817

Blood flow
a noninvasive method to estimate wall shear rate using ultrasound (Brands), 171
an estimation method for blood flow velocity profiles in vessels (Wang), 725
blood perfusion measurement with multifrequency Doppler ultrasound (Eriksson), 49
changes in ultrasonic Doppler backscattered power downstream of concentric and eccentric stenoses under pulsatile flow (Cloutier), 59
Doppler velocity ratio measurements evaluated in a phantom model of multiple arterial disease (Allard), 471
effects of stenosis on transit-time ultrasound measurements of blood flow (Gordon), 623
feasibility study for a two-dimensional diagnostic ultrasound velocity mapping system (Phillips), 217
parameter mapping for the detection of disturbed blood flow (Ferrara), 517
rapid volume flow rate estimation using transverse colour Doppler imaging (Picot), 1199
registration of three-dimensional compound ultrasound scans of the breast for refraction and motion correction (Moskalik), 769
reproducibility of Doppler measurements of blood flow velocity in the uterine and ovarian arteries in premenopausal women (Sladkevicius), 313
segmentation and analysis of colour Doppler images of tumour vasculature (Bell), 635
statistical bias and variance in blood flow estimation by spectral analysis of Doppler signals (Willink), 919
the butterfly search technique for estimation of blood velocity (Alam), 657
the effect of refraction and assumed speeds of sound in tissue and blood on Doppler ultrasound blood velocity measurements (Christopher), 187
the effects of successive high-energy shock-wave tumor administration on tumor blood flow (Cornel), 243
time-domain ultrasonic contrast blood flowmetry (Shung), 71
ultrasonic heating of the brain of the fetal sheep *in utero* (Duggan), 553
vascular resistance quantification in high flow resistance areas using the Doppler method (Arbeille), 321
velocity matched spectrum analysis: a new method for suppressing velocity ambiguity in pulsed-wave Doppler (Torp), 937
volumetric blood flow calculation using a narrow ultrasound beam (Willink), 203

volumetric blood flow measurement by simultaneous Doppler signal and B-mode image processing: a feasibility study (Willink), 481

Blood flow velocity profiles
an estimation method for blood flow velocity profiles in vessels (Wang), 725

Blood group antigens
ffects of ultrasound on agglutination and aggregation of human erythrocytes *in vitro* (Pohl), 711

Blood mimic
acoustic energy determines haemoglobin release from erythrocytes by extracorporeal shock waves *in vitro* (Delius), 707

Blood perfusion
acoustic generation of intra-arterial contrast boluses (Ivey), 757
background subtraction from time-intensity curves in videodensitometry: a pitfall in flow assessment using contrast echocardiography (Bos), 1211
blood perfusion measurement with multifrequency Doppler ultrasound (Eriksson), 49
colour Doppler image analysis for tissue vascularity and perfusion: a preliminary clinical evaluation (Hirsch), 1107
effects of endothelin-1 on renal microvasculature measured using quantitative ultrasound (Insana), 1143
quantification of color Doppler for the evaluation of tissue vascularization (Fein), 1013

Blood rheology
roles of hematocrit and fibrinogen in red cell aggregation determined by ultrasonic scattering properties (Kitamura), 827

Bluth, R. F., see Fleischer, A. C.
Bodard, S., see Arbeille, P.
Bodard, S., see Arbeille, Ph.
Bogdahn, U., see Becker, G.
Bohs, L. N., Friemel, B. H. and Trahey, G. E.: experimental velocity profiles and volumetric flow via two-dimensional speckle tracking, 885
Bom, N., see Pasterkamp, G.
Bom, N., see van der Heiden, M. S.

Bone regeneration
biological effects of shock waves: *in vivo* effect of high energy pulses on rabbit bone (Delius), 1219

Borst, C., see Pasterkamp, G.
Borst, C., see van der Heiden, M. S.
van Bortel, L. M. A. B., see The, S. H. K.
Bos, L. J., Piek, J. J. and Spaan, J. A. E.: background subtraction from time-intensity curves in videodensitometry: a pitfall in flow assessment using contrast echocardiography, 1211
Bouma, C. J., see Pasterkamp, G.
Boving, R., see Delacrétaz, G.
Boving, R., see Pittomvils, G.

BPD (bi-parietal diameter)
scapula length measurement for assessment of fetal growth and development (Dilmen), 139

BPH (benign prostatic hypertrophy)
reproducibility and observer variability of transrectal ultrasound measurements of prostatic volume (Collins), 1101
ultrasound and microbubbles: their generation, detection and potential utilization in tissue and organ therapy—experimental (Fry), 1227
ultrasound focal beam surgery (ter Haar), 1089

Brain
histologic effects of high intensity pulsed ultrasound exposure with subharmonic emission in rabbit brain *in vivo* (Vykhodtseva), 969
preoperative and postoperative follow-up in high-grade gliomas: comparison of transcranial color-coded real-time sonography and computed tomography findings (Becker), 1123
ultrasonic heating of the brain of the fetal sheep *in utero* (Duggan), 553
ultrasound focal beam surgery (ter Haar), 1089

Brain heating
ultrasonic heating of the brain of the fetal sheep *in utero* (Duggan), 553
ultrasound focal beam surgery (ter Haar), 1089

Brain neoplasms
preoperative and postoperative follow-up in high-grade gliomas: comparison of transcranial color-coded real-time sonography and computed tomography findings (Becker), 1123

Brands, P. J., Hoeks, A. P. G. and Reneman, R. S.: the effect of echo suppression on the mean velocity estimation range of the RF cross-correlation model estimator, 945
Brands, P. J., Hoeks, A. P. G., Hofstra, L. and Reneman, R. S.: a noninvasive method to estimate wall shear rate using ultrasound, 171

Breast
a novel ultrasonic technique for differentiating cysts from solid lesions: preliminary results in the breast (Nightingale), 745
preliminary investigation of ultrasound scattering analysis to identify women at risk for later invasive cancer. I: motivation and experimental technique for characterization of isolated breast tissue lobules (Burke), 295
preliminary investigation of ultrasound scattering analysis to identify women at risk for later invasive cancer. II: extraction of dominant scattering angle-dependent trends from excised breast tissue (Burke), 305
registration of three-dimensional compound ultrasound scans of the breast for refraction and motion correction (Moskalik), 769
ultrasound tissue displacement imaging with application to breast cancer (Chen), 1153

Breyer, B., see Heffer-Lauc, M.

Bronchoaerogram
ultrasound imaging of pneumonia (Gehmacher), 1119

Bruce, S., see Loupas, T.

Bubbles (see also Cavitation)
damage to red blood cells induced by acoustic cavitation (Daniels), 105
nonlinear behavior of a liquid containing uniform bubbles: comparison between theory and experiments (Wu), 545
ultrasound contrast agents nucleate inertial cavitation *in vitro* (Miller), 1059
ultrasound focal beam surgery (ter Haar), 1089

Buizza, A., dell'Aquila, T., Giribona, P. and Spagno, C.: the performance of different pressure pulse generators for extracorporeal lithotripsy: a comparison based on commercial lithotripters for kidney stones, 259

Bulk fluid movement
effects of ultrasound on agglutination and aggregation of human erythrocytes *in vitro* (Pohl), 711

Burke, T. M., Blankenberg, T. A., Siu, A. K. Q., Blankenberg, F. G. and Jensen, H. M.: preliminary investigation of ultrasound scattering analysis to identify women at risk for later invasive cancer. I: motivation and experimental technique for characterization of isolated breast tissue lobules, 295

Burke, T. M., Blankenberg, T. A., Siu, A. K. Q., Blankenberg, F. G. and Jensen, H. M.: preliminary investigation of ultrasound scattering analysis to identify women at risk for later invasive cancer. II: extraction of dominant scattering angle-dependent trends from excised breast tissue, 305

Burleson, A. C., N'Guyen, T., Fontaine, A., Levine, R. A. and Yoganathan, A. P.: a model based on dimensional analysis for noninvasive quantification of valvular regurgitation under confined and impinging conditions: *in vitro* pulsatile flow validation, 899

Burns, P. N., see Christopher, D. A.
Buschbom, R. L., see Miller, D. L.
Bush, N. L., see Moran, C. M.

Butterfly search
the butterfly search technique for estimation of blood velocity (Alam), 657

C

Calcification
effect of therapeutic ultrasound on endochondral ossification (Wiltink), 121

Calcium
ultrasonic tissue characterization of end-stage dilated cardiomyopathy (Davison), 853

Calculi
importance of the implosion of ESWL-induced cavitation bubbles (Delacretaz), 97

Campbell, J. S., see Guess, J. F.

Cancer therapy
ultrasound focal beam surgery (ter Haar), 1089

Cancer xenographs
the effects of successive high-energy shock-wave tumor administration on tumor blood flow (Cornel), 243

Cape, E. G., see Fan, P.

Captopril
ultrasonic tissue characterization of end-stage dilated cardiomyopathy (Davison), 853

Cardiac phantom
cardiac ultrasound phantom using a porcine heart model (Smith), 693

Cardiac remodelling
ultrasonic tissue characterization of end-stage dilated cardiomyopathy (Davison), 853

Carnell, M. T. and Emmony, D. C.: a schlieren study of the interaction between a lithotripter shock wave and a simulated kidney stone, 721
Carnes, K. I., Hess, R. A. and Dunn, F.: the effect of ultrasound exposure *in utero* on the development of the fetal mouse testis: adult consequences, 1247

Carotid artery
a noninvasive method to estimate wall shear rate using ultrasound (Brands), 171
diameter and compliance in the human common carotid artery—variations with age and sex (Hansen), 1
Doppler ultrasound spectral shape downstream of significant arterial stenosis *in vivo* (Hutchison), 447
effects of stenosis on transit-time ultrasound measurements of blood flow (Gordon), 623
quantification of intravenous contrast-enhanced Doppler power spectrum in the rabbit carotid artery (Frush), 41
volume flow estimation using time domain correlation and ultrasonic flowmetry (Forsberg), 1037
volumetric blood flow measurement by simultaneous Doppler signal and B-mode image processing: a feasibility study (Willink), 481

Carotid stenosis
effects of stenosis on transit-time ultrasound measurements of blood flow (Gordon), 623

Carson, P. L., see Adler, R. S.
Carson, P. L., see Chen, E. J.
Carson, P. L., see Ivey, J. A.
Carson, P. L., see Moskalik, A.
Carstensen, E. L., see Dalecki, D.

Cartilage
effect of therapeutic ultrasound on endochondral ossification (Wiltink), 121

Cathignol, D., Birer, A., Nachef, S. and Chapelon, J.-Y.: electronic beam steering of shock waves, 365
Cathignol, D., see Delon-Martin, C.

Cavitation
acoustic generation of intra-arterial contrast boluses (Ivey), 757
biological effects of shock waves: *in vivo* effect of high energy pulses on rabbit bone (Delius), 1219
comet assay reveals DNA strand breaks induced by ultrasonic cavitation *in vitro* (Miller), 841
damage to red blood cells induced by acoustic cavitation (Daniels), 105

flow cytometric analysis of cell suspensions exposed to shock waves in the presence of the radical sensitive dye Hydroethidine (Endl), 569
histologic effects of high intensity pulsed ultrasound exposure with subharmonic emission in rabbit brain *in vivo* (Vykhodtseva), 969
importance of the implosion of ESWL-induced cavitation bubbles (Delacretaz), 97
intestinal hemorrhage from exposure to pulsed ultrasound (Dalecki), 1067
macroscopic ESWL-induced cavitation: *in vitro* studies (Pittomvils), 393
the cavitation threshold of human tissue exposed to 0.2-MHz pulsed ultrasound: preliminary measurements based on a study of clinical lithotripsy (Coleman), 405
thresholds for hemorrhages in mouse skin and intestine induced by lithotripter shock waves (Miller), 249
ultrasound and microbubbles: their generation, detection and potential utilization in tissue and organ therapy—experimental (Fry), 1227
ultrasound contrast agents nucleate inertial cavitation *in vitro* (Miller), 1059
venous thrombosis generation by means of high-intensity focused ultrasound (Delon-Martin), 113

Cavitation nucleation
ultrasound contrast agents nucleate inertial cavitation *in vitro* (Miller), 1059

Cavitation threshold
the cavitation threshold of human tissue exposed to 0.2-MHz pulsed ultrasound: preliminary measurements based on a study of clinical lithotripsy (Coleman), 405

Cells
flow cytometric analysis of cell suspensions exposed to shock waves in the presence of the radical sensitive dye Hydroethidine (Endl), 569
physical factors involved in stress-wave-induced cell injury: the effect of stress gradient (Doukas), 961

Cerebral blood flow
assessment of the fetal PO_2 changes by cerebral and umbilical Doppler on lamb fetuses during acute hypoxia (Arbeille), 861
computerised transient hyperaemic response test—a method for the assessment of cerebral autoregulation (Smielewski), 599
is there a hemispheric side preference of cardiac valvular emboli? (Kaps), 753
preoperative and postoperative follow-up in high-grade gliomas: comparison of transcranial color-coded real-time sonography and computed tomography findings (Becker), 1123

Cerebrovascular resistance
computerised transient hyperaemic response test—a method for the assessment of cerebral autoregulation (Smielewski), 599

Céspedes, I., see Ponnekanti, H.
Chapelon, J.-Y., see Cathignol, D.
Chapelon, J. Y., see Delon-Martin, C.
Chen, E. J., Adler, R. S., Carson, P. L., Jenkins, W. K. and O'Brien, W. D. Jr.: ultrasound tissue displacement imaging with application to breast cancer, 1153
Chen, X., see Schwarz, K. Q.

Chi-square distribution
statistical bias and variance in blood flow estimation by spectral analysis of Doppler signals (Willink), 919

Chignier, E., see Delon-Martin, C.
Child, S. Z., see Dalecki, D.
Choi, M. J., see Coleman, A. J.
Christopher, D. A., Burns, P. N., Hunt, J. W. and Foster, F. S.: the effect of refraction and assumed speeds of sound in tissue and blood on Doppler ultrasound blood velocity measurements, 187
Christopher, D. A., see Rickey, D. W.

Chronic pelvic inflammatory disease
the value of transvaginal color Doppler in the assessment of pelvic inflammatory disease (Kupesic), 733

Claes, L., see Augat, P.
Clarke, R. L.: modification of intensity distributions from large aperture ultrasound sources, 353
Cloutier, G., Allard, L. and Durand, L.-G.: changes in ultrasonic Doppler backscattered power downstream of concentric and eccentric stenoses under pulsatile flow, 59
Cloutier, G., see Allard, L.

Clutter suppression
the effect of echo suppression on the mean velocity estimation range of the RF cross-correlation model estimator (Brands), 945

Coleman, A. J., Kodama, T., Choi, M. J., Adams, T. and Saunders, J. E.: the cavitation threshold of human tissue exposed to 0.2-MHz pulsed ultrasound: preliminary measurements based on a study of clinical lithotripsy, 405

Collagen
ultrasonic propagation properties of excised human skin (Moran), 1177

Collins, G. N., Raab, G. M., Hehir, M., King, B. and Garraway, W. M.: reproducibility and observer variability of transrectal ultrasound measurements of prostatic volume, 1101

Colour flow
a numerical and experimental investigation of the flow acceleration region proximal to an orifice (Anayiotos), 501
atrial inflow can alter regurgitant jet size: *in vitro* studies (Grimes), 459
colour Doppler image analysis for tissue vascularity and perfusion: a preliminary clinical evaluation (Hirsch), 1107
Doppler velocity ratio measurements evaluated in a phantom model of multiple arterial disease (Allard), 471
effectiveness of galactose-based intravenous contrast medium on color Doppler sonography of deeply located hepatocellular carcinoma (Tanaka), 157
feasibility study for a two-dimensional diagnostic ultrasound velocity mapping system (Phillips), 217
parameter mapping for the detection of disturbed blood flow (Ferrara), 517
preoperative and postoperative follow-up in high-grade gliomas: comparison of transcranial color-coded real-time sonography and computed tomography findings (Becker), 1123

the butterfly search technique for estimation of blood velocity (Alam), 657
the value of transvaginal color Doppler in the assessment of pelvic inflammatory disease (Kupesic), 733

Colour Doppler
a numerical and experimental investigation of the flow acceleration region proximal to an orifice (Anayiotos), 501
atrial inflow can alter regurgitant jet size: *in vitro* studies (Grimes), 459
colour Doppler image analysis for tissue vascularity and perfusion: a preliminary clinical evaluation (Hirsch), 1107
Doppler velocity ratio measurements evaluated in a phantom model of multiple arterial disease (Allard), 471
effectiveness of galactose-based intravenous contrast medium on color Doppler sonography of deeply located hepatocellular carcinoma (Tanaka), 157
quantification of color Doppler for evaluation of tissue vascularization (Fein), 1013
rapid flow rate estimation using transverse colour Doppler imaging (Picot), 1199
registration of three-dimensional compound ultrasound scans of the breast for refraction and motion correction (Moskalik), 769
segmentation and analysis of colour Doppler images of tumour vasculature (Bell), 635
the butterfly search technique for estimation of blood velocity (Alam), 657
the value of transvaginal color Doppler in the assessment of pelvic inflammatory disease (Kupesic), 733

Colour vector display
experimental velocity profiles and volumetric flow via two-dimensional speckle tracking (Bohs), 885

Comet assay
comet assay reveals DNA strand breaks induced by ultrasonic cavitation *in vitro* (Miller), 841

Comparative study
a survey of the acoustic outputs of diagnostic ultrasound equipment in current clinical use (Henderson), 699
a theory to correct the systematic error caused by the imperfectly matched beam width to vessel diameter ratio on volumetric flow measurements using ultrasound techniques (Fei), 1047
how reliable are manufacturer's reported acoustic output data? (Jago), 135
in situ human obstetrical ultrasound exposimetry: estimates of derating factors for each of three different tissue models (Siddiqi), 379
in vivo comparison of 3D ultrasonography and magnetic resonance imaging in volume estimation of human kidneys (Gilja), 25
preoperative and postoperative follow-up in high-grade gliomas: comparison of transcranial color-coded real-time sonography and computed tomography findings (Becker), 1123
the performance of different pressure pulse generators for extracorporeal lithotripsy: a comparison based on commercial lithotripters for kidney stones (Buizza), 259
validation of transthoracic myocardial ultrasonic tissue characterization: comparison of transthoracic and open-chest measurements of integrated backscatter (Naito), 33

when can Doppler be used in place of integrated backscatter as a measure of scattered ultrasound intensity? (Schwarz), 231

Compliance
assessment of regional vascular distensibility in diseased iliofemoral arteries by intravascular ultrasound (The), 17
diameter and compliance in the human common carotid artery—variations with age and sex (Hansen), 1

Compound scanning
registration of three-dimensional compound ultrasound scans of the breast for refraction and motion correction (Moskalik), 769

Computed tomography
preoperative and postoperative follow-up in high-grade gliomas: comparison of transcranial color-coded real-time sonography and computed tomography findings (Becker), 1123
ultrasound guided percutaneous ethanol treatment of hepatic neoplasms: a therapeutic alternative in the nineties (Bastid), 129

Computer aided diagnosis
computerised transient hyperaemic response test—a method for the assessment of cerebral autoregulation (Smielewski), 599

Computer simulation
comparison of diastolic filling models and their fit to transmitral Doppler contours (Nudelman), 989
experimental velocity profiles and volumetric flow via two-dimensional speckle tracking (Bohs), 885
statistical bias and variance in blood flow estimation by spectral analysis of Doppler signals (Willink), 919
the subtleties of ultrasound images of an ensemble of cells: simulation from regular and more random distributions of scatterers (Hunt), 329
volumetric blood flow calculation using a narrow ultrasound beam (Willink), 203

Confined impinging jets
a model based on dimensional analysis for noninvasive quantification of valvular regurgitation under confined and impinging conditions: *in vitro* pulsatile flow validation (Burleson), 899

Contrast agents
acoustic generation of intra-arterial contrast boluses (Ivey), 757
background subtraction from time-intensity curves in videodensitometry: a pitfall in flow assessment using contrast echocardiography (Bos), 1211
colour Doppler image analysis for tissue vascularity and perfusion: a preliminary clinical evaluation (Hirsch), 1107
effectiveness of galactose-based intravenous contrast medium on color Doppler sonography of deeply located hepatocellular carcinoma (Tanaka), 157
fundamental mechanical limitations on the visualization of elasticity contrast in elastography (Ponnekanti), 533
quantification of intravenous contrast-enhanced Doppler power spectrum in the rabbit carotid artery (Frush), 41
time-domain ultrasonic contrast blood flowmetry (Shung), 71

ultrasound contrast agents nucleate inertial cavitation *in vitro* (Miller), 1059
when can Doppler be used in place of integrated backscatter as a measure of scattered ultrasound intensity? (Schwarz), 231

Contrast enhancement
intravascular ultrasound image subtraction: a contrast enhancing technique to facilitate automatic three-dimensional visualization of the arterial lumen (Pasterkamp), 913

Contrast-transfer efficiency
fundamental mechanical limitations on the visualization of elasticity contrast in elastography (Ponnekanti), 533

Cord compression
assessment of the fetal PO_2 changes by cerebral and umbilical Doppler on lamb fetuses during acute hypoxia (Arbeille), 861

Cornel, E. B., Smits, G. A. H. J., Debruyne, F. M. J., Heerschap, A., Schalken, J. A. and Oosterhof, G. O. N.: the effects of successive high-energy shock-wave tumor administration on tumor blood flow, 243

Correction theory
a wall-less vessel phantom for Doppler ultrasound studies (Rickey), 1163

Counter flow
atrial inflow can alter regurgitant jet size: *in vitro* studies (Grimes), 459

Cox, C., see Francis, C. W.
Cox, G. G., see Insana, M. F.
Crawford, D. C., see Hirsch, W.
Cubberley, F., see Wu, J.
Cullinan, J. A., see Fleischer, A. C.

CW Doppler
assessment of the fetal PO_2 changes by cerebral and umbilical Doppler on lamb fetuses during acute hypoxia (Arbeille), 861
transesophageal color Doppler evaluation of obstructive lesions using the new "Quasar" technology (Fan), 1021

Cyst
a novel ultrasonic technique for differentiating cysts from solid lesions: preliminary results in the breast (Nightingale), 745

Czosnyka, M., see Smielewski, P.

D

Dalecki, D., Raeman, C. H., Child, S. Z. and Carstensen, E. L.: intestinal hemorrhage from exposure to pulsed ultrasound, 1067
Dalecki, D., Raeman, C. H., Child, S. Z. and Carstensen, E. L.: thresholds for intestinal hemorrhage in mice exposed to a piezoelectric lithotripter, 1239
Daminaou, C., see Vykhodtseva, N. I.
Daniels, S., Kodama, T. and Price, D. J.: damage to red blood cells induced by acoustic cavitation, 105
Davison, G., Hall, C. S., Miller, J. G., Scott, M. and Wickline, S. A.: ultrasonic tissue characterization of end-stage dilated cardiomyopathy, 853
Debruyne, F. M. J., see Cornel, E. B.

Decorrelation
ultrasonic estimation of tissue perfusion: a stochastic approach (Adler), 493

Delacrétaz, G., Rink, K., Pittomvils, G., Lafaut, J. P., Vandeursen, H. and Boving, R.: importance of the implosion of ESWL-induced cavitation bubbles, 97

Delius, M., Draenert, K., Al Diek, Y. and Draenert, Y.: biological effects of shock waves: *in vivo* effect of high energy pulses on rabbit bone, 1219

Delius, M., Ueberle, F. and Gambihler, S.: acoustic energy determines haemoglobin release from erythrocytes by extracorporeal shock waves *in vitro*, 707

Delon-Martin, C., Vogt, C., Chignier, E., Guers, C., Chapelon, J. Y. and Cathignol, D.: venous thrombosis generation by means of high-intensity focused ultrasound, 113

Delorme S., see Fein, M.

Derating factor
in situ human obstetrical ultrasound exposimetry: estimates of derating factors for each of three different tissue models (Siddiqi), 379

Dermis
ultrasonic propagation properties of excised human skin (Moran), 1177

Dextran
effects of ultrasound on agglutination and aggregation of human erythrocytes *in vitro* (Pohl), 711

Diastolic dysfunction
assessment of fetal left cardiac isovolumic relaxation time in appropriate and small-for-gestational-age fetuses (Tsyvian), 739

Diastolic function
assessment of fetal left cardiac isovolumic relaxation time in appropriate and small-for-gestational-age fetuses (Tsyvian), 739
comparison of diastolic filling models and their fit to transmitral Doppler contours (Nudelman), 989

Diastolic notch
computer analysis of the early diastolic notch in Doppler sonograms of the uterine arteries (Loupas), 1001

Dichlorofluorescin-diacetate
flow cytometric analysis of cell suspensions exposed to shock waves in the presence of the radical sensitive dye Hydroethidine (Endl), 569

Digital signal processing
the butterfly search technique for estimation of blood velocity (Alam), 657
volumetric blood flow calculation using a narrow ultrasound beam (Willink), 203
volumetric blood flow measurement by simultaneous Doppler signal and B-mode image processing: a feasibility study (Willink), 481

van Dijk, D., see Pasterkamp, G.

Dilmen, G., Öztürk Turhan, N., Fuad Toppare, M., Seçkin, N., Öztürk, M. and Göksin, E.: scapula length measurement for assessment of fetal growth and development, 139

Dimensional analysis
a model based on dimensional analysis for noninvasive quantification of valvular regurgitation under confined and impinging conditions: *in vitro* pulsatile flow validation (Burleson), 899
atrial inflow can alter regurgitant jet size: *in vitro* studies (Grimes), 459

Displacement imaging
ultrasound tissue displacement imaging with application to breast cancer (Chen), 1153

Disturbed blood flow
a model based on dimensional analysis for noninvasive quantification of valvular regurgitation under confined and impinging conditions: *in vitro* pulsatile flow validation (Burleson), 899
effects of stenosis on transit-time ultrasound measurements of blood flow (Gordon), 623
parameter mapping for the detection of disturbed blood flow (Ferrara), 517

DNA
comet assay reveals DNA strand breaks induced by ultrasonic cavitation *in vitro* (Miller), 841
effect of ultrasound on DNA synthesis in tumor cells (Forytková), 585
effects of piezoelectric lithotripsy on human DNA (Bird), 399

DNA damage
comet assay reveals DNA strand breaks induced by ultrasonic cavitation *in vitro* (Miller), 841

DNA repair
comet assay reveals DNA strand breaks induced by ultrasonic cavitation *in vitro* (Miller), 841

DNA synthesis
effect of ultrasound on DNA synthesis in tumor cells (Forytková), 585

Doi, Y., see Naito, J.

Doppler
a model based on dimensional analysis for noninvasive quantification of valvular regurgitation under confined and impinging conditions: *in vitro* pulsatile flow validation (Burleson), 899
a noninvasive method to estimate wall shear rate using ultrasound (Brands), 171
a novel ultrasonic technique for differentiating cysts from solid lesions: preliminary results in the breast (Nightingale), 745
a numerical and experimental investigation of the flow acceleration region proximal to an orifice (Anayiotos), 501
acoustic energy determines haemoglobin release from erythrocytes by extracorporeal shock waves *in vitro* (Delius), 707
adaptive SVD-based AR model order determination for time-frequency analysis of Doppler ultrasound signals (Fort), 793
assessment of fetal left cardiac isovolumic relaxation time in appropriate and small-for-gestational-age fetuses (Tsyvian), 739
assessment of the fetal PO_2 changes by cerebral and umbilical Doppler on lamb fetuses during acute hypoxia (Arbeille), 861
atrial inflow can alter regurgitant jet size: *in vitro* studies (Grimes), 459

bias in mean frequency estimation of Doppler signals due to wall clutter filters (Tysoe), 671
blood perfusion measurement with multifrequency Doppler ultrasound (Eriksson), 49
changes in ultrasonic Doppler backscattered power downstream of concentric and eccentric stenoses under pulsatile flow (Cloutier), 59
comparison of diastolic filling models and their fit to transmitral Doppler contours (Nudelman), 989
correction of intrinsic spectral broadening errors in Doppler peak velocity measurements made with phased sector and linear array transducers (Winkler), 1029
demonstration of three-dimensional vector flow estimation using bandwidth and two transducers on a flow phantom (McArdle), 679
Doppler ultrasound spectral shape downstream of significant arterial stenosis *in vivo* (Hutchison), 447
Doppler velocity ratio measurements evaluated in a phantom model of multiple arterial disease (Allard), 471
effectiveness of galactose-based intravenous contrast medium on color Doppler sonography of deeply located hepatocellular carcinoma (Tanaka), 157
effects of endothelin-1 on renal microvasculature measured using quantitative ultrasound (Insana), 1143
effects of nonuniform insonation by catheter-tipped Doppler transducers on velocity estimation (Moraes), 779
experimental velocity profiles and volumetric flow via two-dimensional speckle tracking (Bohs), 885
feasibility study for a two-dimensional diagnostic ultrasound velocity mapping system (Phillips), 217
glycoprotein and ganglioside changes in human trophoblasts after exposure to pulsed Doppler ultrasound (Heffer-Lauc), 579
improved blood velocity estimation using the maximum Doppler frequency (Tortoli), 527
monitoring intracranial dynamics by transcranial Doppler—a new Doppler index: trans systolic time (Hanlo), 613
parameter mapping for the detection of disturbed blood flow (Ferrara), 517
preoperative and postoperative follow-up in high-grade gliomas: comparison of transcranial color-coded real-time sonography and computed tomography findings (Becker), 1123
quantification of color Doppler for the evaluation of tissue vascularization (Fein), 1013
quantification of intravenous contrast-enhanced Doppler power spectrum in the rabbit carotid artery (Frush), 41
quantitative investigation of *in vitro* flow using three-dimensional colour Doppler ultasound (Guo), 807
rapid volume flow rate estimation using transverse colour Doppler imaging (Picot), 1199
registration of three-dimensional compound ultrasound scans of the breast for refraction and motion correction (Moskalik), 769
reproducibility of Doppler measurements of blood flow velocity in the uterine and ovarian arteries in premenopausal women (Sladkevicius), 313
segmentation and analysis of colour Doppler images of tumour vasculature (Bell), 635
serial assessment of adnexal masses with transvaginal color Doppler sonography (Fleischer), 435

statistical bias and variance in blood flow estimation by spectral analysis of Doppler signals (Willink), 919
the butterfly search technique for estimation of blood velocity (Alam), 657
the effect of refraction and assumed speeds of sound in tissue and blood on Doppler ultrasound blood velocity measurements (Christopher), 187
the value of transvaginal color Doppler in the assessment of pelvic inflammatory disease (Kupesic), 733
time-domain ultrasonic contrast blood flowmetry (Shung), 71
ultrasonic estimation of tissue perfusion: a stochastic approach (Adler), 493
ultrasonic heating of the brain of the fetal sheep *in utero* (Duggan), 553
umbilical cord venous pulsation in normal fetuses and its incidence after 13 weeks of gestation (Nakai), 443
vascular resistance quantification in high flow resistance areas using the Doppler method (Arbeille), 321
volumetric blood flow calculation using a narrow ultrasound beam (Willink), 203
volumetric blood flow measurement by simultaneous Doppler signal and B-mode image processing: a feasibility study (Willink), 481
when can Doppler be used in place of integrated backscatter as a measure of scattered ultrasound intensity? (Schwarz), 231

Doppler angle
a noninvasive method to estimate wall shear rate using ultrasound (Brands), 171
correction of intrinsic spectral broadening errors in Doppler peak velocity measurements made with phased sector and linear array transducers (Winkler), 1029

Doppler heating
ultrasonic heating of the brain of the fetal sheep *in utero* (Duggan), 553

Doppler index
assessment of the fetal PO_2 changes by cerebral and umbilical Doppler on lamb fetuses during acute hypoxia (Arbeille), 861
monitoring intracranial dynamics by transcranial Doppler—a new Doppler index: trans systolic time (Hanlo), 613

Doppler parameters
vascular resistance quantification in high flow resistance areas using the Doppler method (Arbeille), 321

Doppler power
changes in ultrasonic Doppler backscattered power downstream of concentric and eccentric stenoses under pulsatile flow (Cloutier), 59

Doppler power ratio
quantification of intravenous contrast-enhanced Doppler power spectrum in the rabbit carotid artery (Frush), 41

Doppler spectrum
improved blood velocity estimation using the maximum Doppler frequency (Tortoli), 527

Doppler waveform analysis
computer analysis of the early diastolic notch in Doppler sonograms of the uterine arteries (Loupas), 1001

Dosimetry
in situ human obstetrical ultrasound exposimetry: estimates of derating factors for each of three different tissue models (Siddiqi), 379

Doukas, A. G., McAuliffe, D. J., Lee, S., Venugopalan, V. and Flotte T. J.: physical factors involved in stress-wave-induced cell injury: the effect of stress gradient, 961
Draenert, K., see Delius, M.
Draenert, Y., see Delius, M.
Du, G., see Wu, J.
Duggan, P. M., Liggins, G. C. and Barnett, S. B.: ultrasonic heating of the brain of the fetal sheep *in utero*, 553
Dunn, F., see Carnes, K. I.
Durand, L.-G., see Allard, L.
Durand, L.-G., see Cloutier, G.
Dymling, S. O., see Eriksson, R.

E

Echo enhancement
quantification of intravenous contrast-enhanced Doppler power spectrum in the rabbit carotid artery (Frush), 41

Echocardiography
a numerical and experimental investigation of the flow acceleration region proximal to an orifice (Anayiotos), 501
background subtraction from time-intensity curves in videodensitometry: a pitfall in flow assessment using contrast echocardiography (Bos), 1211
cardiac ultrasound phantom using a porcine heart model (Smith), 693
comparison of diastolic filling models and their fit to transmitral Doppler contours (Nudelman), 989
transesophageal color Doppler evaluation of obstructive lesions using the new "Quasar" technology (Fan), 1021
ultrasonic three-dimensional reconstruction of the heart (Salustri), 281 (Review)
validation of transthoracic myocardial ultrasonic tissue characterization: comparison of transthoracic and open-chest measurements of integrated backscatter (Naito), 33
when can Doppler be used in place of integrated backscatter as a measure of scattered ultrasound intensity? (Schwarz), 231

Echogenicity
echogenicity of experimental liver ethanol injections (Vehmas), 1137

Eckersley, R. J., see Bell, D. S.
Eddy, H. A., see Harrison, G. H.

Ehrlich ascitic tumour
effect of ultrasound on DNA synthesis in tumor cells (Forytková), 585

Elasticity
diameter and compliance in the human common carotid artery—variations with age and sex (Hansen), 1

Elasticity imaging
elasticity imaging for early detection of renal pathology (Emelianov), 871

Elastogram
fundamental mechanical limitations on the visualization of elasticity contrast in elastography (Ponnekanti), 533

Elastography
elasticity imaging for early detection of renal pathology (Emelianov), 871
fundamental mechanical limitations on the visualization of elasticity contrast in elastography (Ponnekanti), 533
ultrasound tissue displacement imaging with application to breast cancer (Chen), 1153

Ellis, D. S., see Tarantal, A. F.
Ellwood, D. A., see Loupas, T.

Embolic stroke
is there a hemispheric side preference of cardiac valvular emboli? (Kaps), 753

Emelianov, S. Y., Lubinski, M. A., Weitzel, W. F., Wiggins, R. C., Skovoroda, A. R. and O'Donnell, M.: elasticity imaging for early detection of renal pathology, 871
Emmony, D. C., see Carnell, M. T.

Endarterectomy
effects of stenosis on transit-time ultrasound measurements of blood flow (Gordon), 623

Endl, E., Steinbach, P. and Hofstädter, F.: flow cytometric analysis of cell suspensions exposed to shock waves in the presence of the radical sensitive dye Hydroethidine, 569

Endochondral ossification
effect of therapeutic ultrasound on endochondral ossification (Wiltink), 121

Endothelin
effects of endothelin-1 on renal microvasculature measured using quantitative ultrasound (Insana), 1143

Endothelium
venous thrombosis generation by means of high-intensity focused ultrasound (Delon-Martin), 113

Enhancement
effectiveness of galactose-based intravenous contrast medium on color Doppler sonography of deeply located hepatocellular carcinoma (Tanaka), 157

Ensemble averaging
computer analysis of the early diastolic notch in Doppler sonograms of the uterine arteries (Loupas), 1001

Epidermis
ultrasonic propagation properties of excised human skin (Moran), 1177

Eriksson, R., Persson, H.W., Dymling, S.O. and Lindström, K.: blood perfusion measurement with multifrequency Doppler ultrasound, 49

Errors
a wall-less vessel phantom for Doppler ultrasound studies (Rickey), 1163
bias in mean frequency estimation of Doppler signals due to wall clutter filters (Tysoe), 671
correction of intrinsic spectral broadening errors in Doppler peak velocity measurements made with phased sector and linear array transducers (Winkler), 1029
errors in transrectal ultrasonic planimetry of the prostate: computer simulation of volumetric errors applied to a screening population (Bangma), 11
errors in transrectal ultrasonic planimetry of the prostate: computer simulation of volumetric errors applied to a screening population: regarding Bangma et al. UMB 21(1):11–16; 1995 (Aarnink), 1083
improved blood velocity estimation using the maximum Doppler frequency (Tortoli), 527
reproducibility and observer variability of transrectal ultrasound measurements of prostatic volume (Collins), 1101
reproducibility of Doppler measurements of blood flow velocity in the uterine and ovarian arteries in premenopausal women (Sladkevicius), 313
statistical bias and variance in blood flow estimation by spectral analysis of Doppler signals (Willink), 919
the effect of echo suppression on the mean velocity estimation range of the RF cross-correlation model estimator (Brands), 945
the effect of refraction and assumed speeds of sound in tissue and blood on Doppler ultrasound blood velocity measurements (Christopher), 187
ultrasonic propagation properties of excised human skin (Moran), 1177

Erythrocyte membrane
effects of ultrasound on agglutination and aggregation of human erythrocytes *in vitro* (Pohl), 711

Erythrocytes
acoustic energy determines haemoglobin release from erythrocytes by extracorporeal shock waves *in vitro* (Delius), 707
effects of ultrasound on agglutination and aggregation of human erythrocytes *in vitro* (Pohl), 711
roles of hematocrit and fibrinogen in red cell aggregation determined by ultrasonic scattering properties (Kitamura), 827
ultrasound backscatter at 30 MHz from human blood: influence of rouleau size affected by blood modification and shear rate (van der Heiden), 817

ESWL (extracorporeal shock wave lithotripsy)
a Schlieren study of the interaction between a lithotripter shock wave and a simulated kidney stone (Carnell), 721
acoustic energy determines haemoglobin release from erythrocytes by extracorporeal shock waves *in vitro* (Delius), 707
biological effects of shock waves: *in vivo* effect of high energy pulses on rabbit bone (Delius), 1219
effects of piezoelectric lithotripsy on human DNA (Bird), 399
electronic beam steering of shock waves (Cathignol), 365
flow cytometric analysis of cell suspensions exposed to shock waves in the presence of the radical sensitive dye Hydroethidine (Endl), 569

importance of the implosion of ESWL-induced cavitation bubbles (Delacretaz), 97
influence of water temperature on pressure pulses generated by an electromagnetic type lithotripter (Augat), 89
macroscopic ESWL-induced cavitation: *in vitro* studies (Pittomvils), 393
the cavitation threshold of human tissue exposed to 0.2-MHz pulsed ultrasound: preliminary measurements based on a study of clinical lithotripsy (Coleman), 405
the performance of different pressure pulse generators for extracorporeal lithotripsy: a comparison based on commercial lithotripters for kidney stones (Buizza), 259
thresholds for hemorrhages in mouse skin and intestine induced by lithotripter shock waves (Miller), 249
thresholds for intestinal hemorrhage in mice exposed to a piezoelectric lithotripter (Dalecki), 1239

Ethanol
echogenicity of experimental liver ethanol injections (Vehmas), 1137

Evans, D. H., see Moraes, R.
Evans, D. H., see Tysoe, C.
Evans, D. H., see Willink, R.

Exposimetry
in situ human obstetrical ultrasound exposimetry: estimates of derating factors for each of three different tissue models (Siddiqi), 379
the effect of ultrasound exposure *in utero* on the development of the fetal mouse testis: adult consequences (Carnes), 1247

Exposure criteria
exposure criteria for medical diagnostic ultrasound: I. criteria based on thermal mechanisms (Jago), 425 (Book Review)

F

Fan, P., Nanda, N. C., Gatewood, R. P., Jr., Cape, E. G. and Yoganathan, A. P.: transesophageal color Doppler evaluation of obstructive lesions using the new "Quasar" technology, 1021
Fan, P. H., see Anayiotos, A. S.

Fat
ultrasonic propagation properties of excised human skin (Moran), 1177

Fatkin, D., Loupas, T., Jacobs, N. and Feneley, M. P.: quantification of blood echogenicity: evaluation of a semiquantitative method of grading spontaneous echo contrast, 1191
Fay, R. A., see Loupas, T.
Fei, D. Y.: a theory to correct the systematic error caused by the imperfectly matched beam width to vessel diameter ratio on volumetric flow measurements using ultrasound techniques, 1047
Fein, M., Delorme S., Weisser, G., Zuna, I. and van Kaick, G.: quantification of color Doppler for the evaluation of tissue vascularization, 1013
Feleppa, E. J., see Kitamura, H.

Femoral artery
rapid volume flow rate estimation using transverse colour Doppler imaging (Picot), 1199

vascular resistance quantification in high flow resistance areas using the Doppler method (Arbeille), 321
volume flow estimation using time domain correlation and ultrasonic flowmetry (Forsberg), 1037
volumetric blood flow calculation using a narrow ultrasound beam (Willink), 203

Femoral vein
venous thrombosis generation by means of high-intensity focused ultrasound (Delon-Martin), 113

Femur length
scapula length measurement for assessment of fetal growth and development (Dilmen), 139

Feneley, M. P., see Fatkin, D.
Fenster, A., see Guo, Z.
Fenster, A., see Picot, P. A.
Fenster, A., see Rickey, D. W.
Ferrara, K. W., Ostromogilsky, M., Rosenberg, S. and Sokil-Melgar, J.: parameter mapping for the detection of disturbed blood flow, 517

Fetal cardiac isovolumic relaxation
assessment of fetal left cardiac isovolumic relaxation time in appropriate and small-for-gestational-age fetuses (Tsyvian), 739

Fetal development
scapula length measurement for assessment of fetal growth and development (Dilmen), 139

Fetal measurements
scapula length measurement for assessment of fetal growth and development (Dilmen), 139
umbilical cord venous pulsation in normal fetuses and its incidence after 13 weeks of gestation (Nakai), 443

Fetal sheep
ultrasonic heating of the brain of the fetal sheep *in utero* (Duggan), 553

Fetus
hematologic and growth-related effects of frequent prenatal ultrasound exposure in the long-tailed macaque (macaca fascicularis) (Tarantal), 1073
scapula length measurement for assessment of fetal growth and development (Dilmen), 139
ultrasonic heating of the brain of the fetal sheep *in utero* (Duggan), 553
umbilical cord venous pulsation in normal fetuses and its incidence after 13 weeks of gestation (Nakai), 443

de Feyter, P., see The, S. H. K.

Fibrinogen
roles of hematocrit and fibrinogen in red cell aggregation determined by ultrasonic scattering properties (Kitamura), 827

Fibrinolysis
pro- and antifibrinolytic effects of ultrasound on streptokinase-induced thrombolysis (Nilsson), 833

ultrasound accelerates transport of recombinant tissue plasminogen activator into clots (Francis), 419

Fignon, A., see Arbeille, P.

Finite element analysis
fundamental mechanical limitations on the visualization of elasticity contrast in elastography (Ponnekanti), 533
parameter mapping for the detection of disturbed blood flow (Ferrara), 517

Fleischer, A. C., Cullinan, J. A., Jones, H. W., III, Peery, C. V., Bluth, R. F. and Kepple, D. M.: serial assessment of adnexal masses with transvaginal color Doppler sonography, 435
Flenniken, R. R., see Shung, K. K.
Flögel, M., see Heffer-Lauc, M.
Flotte T. J., see Doukas, A. G.

Flow
a model based on dimensional analysis for noninvasive quantification of valvular regurgitation under confined and impinging conditions: *in vitro* pulsatile flow validation (Burleson), 899
a noninvasive method to estimate wall shear rate using ultrasound (Brands), 171
a numerical and experimental investigation of the flow acceleration region proximal to an orifice (Anayiotos), 501
a wall-less vessel phantom for Doppler ultrasound studies (Rickey), 1163
acoustic energy determines haemoglobin release from erythrocytes by extracorporeal shock waves *in vitro* (Delius), 707
atrial inflow can alter regurgitant jet size: *in vitro* studies (Grimes), 459
blood perfusion measurement with multifrequency Doppler ultrasound (Eriksson), 49
changes in ultrasonic Doppler backscattered power downstream of concentric and eccentric stenoses under pulsatile flow (Cloutier), 59
correction of intrinsic spectral broadening errors in Doppler peak velocity measurements made with phased sector and linear array transducers (Winkler), 1029
demonstration of three-dimensional vector flow estimation using bandwidth and two transducers on a flow phantom (McArdle), 679
Doppler ultrasound spectral shape downstream of significant arterial stenosis *in vivo* (Hutchison), 447
Doppler velocity ratio measurements evaluated in a phantom model of multiple arterial disease (Allard), 471
effects of stenosis on transit-time ultrasound measurements of blood flow (Gordon), 623
experimental velocity profiles and volumetric flow via two-dimensional speckle tracking (Bohs), 885
parameter mapping for the detection of disturbed blood flow (Ferrara), 517
quantitative investigation of *in vitro* flow using three-dimensional colour Doppler ultrasound (Guo), 807
rapid volume flow rate estimation using transverse colour Doppler imaging (Picot), 1199
reproducibility of Doppler measurements of blood flow velocity in the uterine and ovarian arteries in premenopausal women (Sladkevicius), 313
segmentation and analysis of colour Doppler images of tumour vasculature (Bell), 635

statistical bias and variance in blood flow estimation by spectral analysis of Doppler signals (Willink), 919
the butterfly search technique for estimation of blood velocity (Alam), 657
time-domain ultrasonic contrast blood flowmetry (Shung), 71
transesophageal color Doppler evaluation of obstructive lesions using the new "Quasar" technology (Fan), 1021
ultrasonic estimation of tissue perfusion: a stochastic approach (Adler), 493
velocity matched spectrum analysis: a new method for suppressing velocity ambiguity in pulsed-wave Doppler (Torp), 937
when can Doppler be used in place of integrated backscatter as a measure of scattered ultrasound intensity? (Schwarz), 231

Flow acceleration
a numerical and experimental investigation of the flow acceleration region proximal to an orifice (Anayiotos), 501

Flow cytometry
flow cytometric analysis of cell suspensions exposed to shock waves in the presence of the radical sensitive dye Hydroethidine (Endl), 569

Flow phantom
a model based on dimensional analysis for noninvasive quantification of valvular regurgitation under confined and impinging conditions: *in vitro* pulsatile flow validation (Burleson), 899
a numerical and experimental investigation of the flow acceleration region proximal to an orifice (Anayiotos), 501
acoustic energy determines haemoglobin release from erythrocytes by extracorporeal shock waves *in vitro* (Delius), 707
atrial inflow can alter regurgitant jet size: *in vitro* studies (Grimes), 459
blood perfusion measurement with multifrequency Doppler ultrasound (Eriksson), 49
changes in ultrasonic Doppler backscattered power downstream of concentric and eccentric stenoses under pulsatile flow (Cloutier), 59
correction of intrinsic spectral broadening errors in Doppler peak velocity measurements made with phased sector and linear array transducers (Winkler), 1029
demonstration of three-dimensional vector flow estimation using bandwidth and two transducers on a flow phantom (McArdle), 679
Doppler velocity ratio measurements evaluated in a phantom model of multiple arterial disease (Allard), 471
effects of stenosis on transit-time ultrasound measurements of blood flow (Gordon), 623
parameter mapping for the detection of disturbed blood flow (Ferrara), 517
quantitative investigation of *in vitro* flow using three-dimensional colour Doppler ultrasound (Guo), 807
rapid volume flow rate estimation using transverse colour Doppler imaging (Picot), 1199
the butterfly search technique for estimation of blood velocity (Alam), 657
time-domain ultrasonic contrast blood flowmetry (Shung), 71
transesophageal color Doppler evaluation of obstructive lesions using the new "Quasar" technology (Fan), 1021
ultrasonic estimation of tissue perfusion: a stochastic approach (Adler), 493
when can Doppler be used in place of integrated backscatter as a measure of scattered ultrasound intensity? (Schwarz), 231

Flow profile
quantitative investigation of *in vitro* flow using three-dimensional colour Doppler ultrasound (Guo), 807

Flow quantification
experimental velocity profiles and volumetric flow via two-dimensional speckle tracking (Bohs), 885

Flow separation
Doppler ultrasound spectral shape downstream of significant arterial stenosis *in vivo* (Hutchison), 447

Flow velocity
a noninvasive method to estimate wall shear rate using ultrasound (Brands), 171
experimental velocity profiles and volumetric flow via two-dimensional speckle tracking (Bohs), 885
reproducibility of Doppler measurements of blood flow velocity in the uterine and ovarian arteries in premenopausal women (Sladkevicius), 313

Flow visualization
quantitative investigation of *in vitro* flow using three-dimensional colour of Doppler ultrasound (Guo), 807

Flurocarbon
quantification of intravenous contrast-enhanced Doppler power spectrum in the rabbit carotid artery (Frush), 41

Fobbe, F., see Hamm, B.

Focal ultrasound
ultrasound focal beam surgery (ter Haar), 1089

Focusing
influence of water temperature on pressure pulses generated by an electromagnetic type lithotripter (Augat), 89
modification of intensity distributions from large aperture ultrasound sources (Clarke), 353
ultrasound focal beam surgery (ter Haar), 1089
venous thrombosis generation by means of high-intensity focused ultrasound (Delon-Martin), 113

Fontaine, A., see Burleson, A. C.
Forsberg, F., Liu, J.-B., Russell, K. M., Guthrie, S. L. and Goldberg, B. B.: volume flow estimation using time domain correlation and ultrasonic flowmetry, 1037
Fort, A., Manfredi, C. and Rocchi, S.: adaptive SVD-based AR model order determination for time-frequency analysis of Doppler ultrasound signals, 793
Forytková, L., Hrazdira, I. and Mornstein, V.: effect of ultrasound on DNA synthesis in tumor cells, 585
Foster, F. S., see Christopher, D. A.
Foster, F. S., see Turnbull, D. H.
Foster, R. S., see Fry, F. J.

Fourier analysis
acoustic properties of some biocompatible polymers at body temperature (Guess), 273
statistical bias and variance in blood flow estimation by spectral analysis of Doppler signals (Willink), 919
volumetric blood flow calculation using a narrow ultrasound beam (Willink), 203

Fowlkes, J. B., see Adler, R. S.
Fowlkes, J. B., see Ivey, J. A.
Fowlkes, J. B., see Moskalik, A.
Francis, C. W., Blinc, A., Lee, S. and Cox, C.: ultrasound accelerates transport of recombinant tissue plasminogen activator into clots, 419

Free radicals
flow cytometric analysis of cell suspensions exposed to shock waves in the presence of the radical sensitive dye Hydroethidine (Endl), 569

Friemel, B. H., see Bohs, L. N.
From, L., see Turnbull, D. H.
Fruitman, M., see Picot, P. A.
Frush, D. P., Babcock, D. S., White, K. S. and Barr, L. L.: quantification of intravenous contrast-enhanced Doppler power spectrum in the rabbit carotid artery, 41
Fry, F. J.: comparison of ultrasound irradiation of pregnant mice with other bioeffects data, 430
Fry, F. J., Sanghvi, N. T., Foster, R. S., Bihrle, R. and Hennige C.: ultrasound and microbubbles: their generation, detection and potential utilization in tissue and organ therapy—experimental, 1227
Fuad Toppare, M., see Dilmen, G.

Fundamental limits
fundamental mechanical limitations on the visualization of elasticity contrast in elastography (Ponnekanti), 533

G

Gahn, G., see Becker, G.

Gall bladder
effects of piezoelectric lithotripsy on human DNA (Bird), 399

Gallstones
effects of piezoelectric lithotripsy on human DNA (Bird), 399
ultrasound and microbubbles: their generation, detection and potential utilization in tissue and organ therapy—experimental (Fry), 1227

Gambihler, S., see Delius, M.

Gangliosides
glycoprotein and ganglioside changes in human trophoblasts after exposure to pulsed Doppler ultrasound (Heffer-Lauc), 579

Gardner, E. A., see Ivey, J. A.
Gargosky, S. E., see Tarantal, A. F.
Garraway, W. M., see Collins, G. N.
Gatewood, R. P. Jr., see Fan, P.

Gehmacher, O., Kopf, G. M. A. and Scheier, M.: ultrasound imaging of pneumonia, 1119

Geonotoxicity
effects of piezoelectric lithotripsy on human DNA (Bird), 399

Gilja, O. H., Smievoll, A. I., Thune, N., Matre, K., Hausken, T., Odegaard, S. and Berstad, A.: *in vivo* comparison of 3D ultrasonography and magnetic resonance imaging in volume estimation of human kidneys, 25
Gill, R. W., see Loupas, T.
Giribona, P., see Buizza, A.

Glioma
preoperative and postoperative follow-up in high-grade gliomas: comparison of transcranial color-coded real-time sonography and computed tomography findings (Becker), 1123

Glycoproteins
glycoprotein and ganglioside changes in human trophoblasts after exposure to pulsed Doppler ultrasound (Heffer-Lauc), 579

Göksin, E., see Dilmen, G.
Goldberg, B. B., see Forsberg, F.
Gooskens, R. H. J. M., see Hanlo, P. W.
Gordon, I. L.: effects of stenosis on transit-time ultrasound measurements of blood flow, 623
Gormley, G., see Wu, J.
Green, D. W., see Anayiotos, A. S.
Grimes, R. Y., Nyarko, S. J., Pulido, G. A., Yang, S., Walker, P. G., Levine, R. A. and Yoganathan, A. P.: atrial inflow can alter regurgitant jet size: *in vitro* studies, 459
Guers, C., see Delon-Martin, C.
Guess, J. F. and Campbell, J. S.: acoustic properties of some biocompatible polymers at body temperature, 273

Guidance
ultrasound guided percutaneous ethanol treatment of hepatic neoplasms: a therapeutic alternative in the nineties (Bastid), 129 (CN)
ultrasound-guided microwave thermotherapy on a VX-2 carcinoma implanted in rabbit kidney (Kigure), 649

Guidi, G., see Tortoli, P.
Guo, Z., Moreau, M., Rickey, D. W., Picot, P. A. and Fenster, A.: quantitative investigation of *in vitro* flow using three-dimensional colour Doppler ultrasound, 807
Gupta, A. K., see Turnbull, D. H.
Gussenhoven, E. J., see Pasterkamp, G.
Gussenhoven, E. J., see The, S. H. K.
Guthrie, S. L., see Forsberg, F.

Gynaecology
the value of transvaginal color Doppler in the assessment of pelvic inflammatory disease (Kupesic), 733

H

ter Haar, G.: ultrasound focal beam surgery, 1089
ter Haar Romeny, B. M., see Pasterkamp, G.

Haemoglobin
damage to red blood cells induced by acoustic cavitation (Daniels), 105

Haemolysis
acoustic energy determines haemoglobin release from erythrocytes by extracorporeal shock waves *in vitro* (Delius), 707
damage to red blood cells induced by acoustic cavitation (Daniels), 105

Haemorrhagic necrosis
ultrasound focal beam surgery (ter Haar), 1089

Hall, A. F., see Nudelman, S.
Hall, C. S., see Davison, G.
Hall, T. J., see Insana, M. F.
Hamm, B. and Fobbe, F.: maturation of the testis: ultrasound evaluation, 143

Hamster
ultrasonic tissue characterization of end-stage dilated cardiomyopathy (Davison), 853

Hanlo, P. W., Peters, R. J. A., Gooskens, R. H. J. M., Heethaar, R. M., Keunen, R. W. M., van Huffelen, A. C., Tulleken, C. A. F. and Willemse, J.: monitoring intracranial dynamics by transcranial Doppler—a new Doppler index: trans systolic time, 613
Hansen, F., Mangell, P., Sonesson, B. and Länne, T.: diameter and compliance in the human common carotid artery—variations with age and sex, 1
Harada, T., see Kigure, T.
Harasiewicz, K. A., see Turnbull, D. H.
Harrison, G. H., Eddy, H. A., Wang, J.-P. and Liberman, F. Z.: microscopic lung alterations and reduction of respiration rate in insonated anesthetized swine, 981
Harrison, L. A., see Insana, M. F.
Hausken, T., see Gilja, O. H.

Hazard
physical factors involved in stress-wave-induced cell injury: the effect of stress gradient (Doukas), 961

Heart
assessment of fetal left cardiac isovolumic relaxation time in appropriate and small-for-gestational-age fetuses (Tsyvian), 739
cardiac ultrasound phantom using a porcine heart model (Smith), 693
ultrasonic tissue characterization of end-stage dilated cardiomyopathy (Davison), 853

Heating
damage to red blood cells induced by acoustic cavitation (Daniels), 105
hematologic and growth-related effects of frequent prenatal ultrasound exposure in the long-tailed macaque (macaca fascicularis) (Tarantal), 1073
intestinal hemorrhage from exposure to pulsed ultrasound (Dalecki), 1067
modification of intensity distributions from large aperture ultrasound sources (Clarke), 353
temperature rise generated by diagnostic ultrasound in a transcranial phantom (Wu), 561

ultrasonic heating of the brain of the fetal sheep *in utero* (Duggan), 553
ultrasound focal beam surgery (ter Haar), 1089
ultrasound-guided microwave thermotherapy on a VX-2 carcinoma implanted in rabbit kidney (Kigure), 649

Heerschap, A., see Cornel, E. B.
Heethaar, R. M., see Hanlo, P. W.
Heffer-Lauc, M., Latin, V., Breyer, B., Flögel, M., Müller, W. E. G. and Lauc, G.: glycoprotein and ganglioside changes in human trophoblasts after exposure to pulsed Doppler ultrasound, 579
Hehir, M., see Collins, G. N.
van der Heiden, M. S., de Kroon, M. G. M., Bom, N. and Borst, C.: ultrasound backscatter at 30 MHz from human blood: influence of rouleau size affected by blood modification and shear rate, 817
van der Heiden, M. S., see Pasterkamp, G.
Hekkenberg, R. T., see Wiltink, A.
Helders, P. J. M., see Wiltink, A.

Hematocrit
roles of hematocrit and fibrinogen in red cell aggregation determined by ultrasonic scattering properties (Kitamura), 827

Hematopoiesis
hematologic and growth-related effects of frequent prenatal ultrasound exposure in the long-tailed macaque (macaca fascicularis) (Tarantal), 1073

Hemodynamics
a numerical and experimental investigation of the flow acceleration region proximal to an orifice (Anayiotos), 501
Doppler velocity ratio measurements evaluated in a phantom model of multiple arterial disease (Allard), 471

Hemorrhage
thresholds for hemorrhages in mouse skin and intestine induced by lithotripter shock waves (Miller), 249

Henderson, J., see Jago, J. R.
Henderson, J., Willson, K., Jago, J. R. and Whittingham, T. A.: a survey of the acoustic outputs of diagnostic ultrasound equipment in current clinical use, 699
Hendrickx, A. G., see Tarantal, A. F.
Hengeveld, E. J., see Bangma, C. H.
Hennige C., see Fry, F. J.
Hess, R. A., see Carnes, K. I.

Hepatocellular carcinoma
effectiveness of galactose-based intravenous contrast medium on color Doppler sonography of deeply located hepatocellular carcinoma (Tanaka), 157
ultrasound guided percutaneous ethanol treatment of hepatic neoplasms: a therapeutic alternative in the nineties (Bastid), 129 (CN)

Hete, B. and Shung, K. K.: a study of the relationship between mechanical and ultrasonic properties of dystrophic and normal skeletal muscle, 343

HIFU (high intensity focused ultrasound), see also ESWL
electronic beam steering of shock waves (Cathignol), 365

histologic effects of high intensity pulsed ultrasound exposure with subharmonic emission in rabbit brain *in vivo* (Vykhodtseva), 969
ultrasound focal beam surgery (ter Haar), 1089
venous thrombosis generation by means of high-intensity focused ultrasound (Delon-Martin), 113

High energy shock waves
a Schlieren study of the interaction between a lithotripter shock wave and a simulated kidney stone (Carnell), 721
effects of piezoelectric lithotripsy on human DNA (Bird), 399
electronic beam steering of shock waves (Cathignol), 365
flow cytometric analysis of cell suspensions exposed to shock waves in the presence of the radical sensitive dye Hydroethidine (Endl), 569
importance of the implosion of ESWL-induced cavitation bubbles (Delacretaz), 97
influence of water temperature on pressure pulses generated by an electromagnetic type lithotripter (Augat), 89
macroscopic ESWL-induced cavitation: *in vitro* studies (Pittomvils), 393
the cavitation threshold of human tissue exposed to 0.2-MHz pulsed ultrasound: preliminary measurements based on a study of clinical lithotripsy (Coleman), 405
the effects of successive high-energy shock-wave tumor administration on tumor blood flow (Cornel), 243
the performance of different pressure pulse generators for extracorporeal lithotripsy: a comparison based on commercial lithotripters for kidney stones (Buizza), 259
thresholds for hemorrhages in mouse skin and intestine induced by lithotripter shock waves (Miller), 249
thresholds for intestinal hemorrhage in mice exposed to a piezoelectric lithotripter (Dalecki), 1239

High frequency
a 40–100 MHz B-scan ultrasound backscatter microscope for skin imaging (Turnbull), 79
ultrasound backscatter at 30 MHz from human blood: influence of rouleau size affected by blood modification and shear rate (van der Heiden), 817

High resistance index
vascular resistance quantification in high flow resistance areas using the Doppler method (Arbeille), 321

Hirsch, W., Bell, D. S., Crawford, D. C., Kale S. G., McCready, V. R. and Bamber, J. C.: colour Doppler image analysis for tissue vascularity and perfusion: a preliminary clinical evaluation, 1107
Hoeks, A. P. G. see Brands, P. J.
Hofmann, E., see Becker, G.
Hofstädter, F., see Endl, E.
Hofstra, L., see Brands, P. J.
Holden, J. E. and Madsen, E. L.: foundations of medical imaging, 133 (Book Review)
Hori, M., see Naito, J.
Hrazdira, I., see Forytková, L.
Hrazdira, I., Sulcova, A., Kellnerova, R. and Huskova, B.: prenatal application of diagnostic ultrasound in mice, 427
Huang, Y., see Ponnekanti, H.

van Huffelen, A. C., see Hanlo, P. W.
Hunt, J. W., see Christopher, D. A.
Hunt, J. W., Worthington, A. E. and Kerr, A. T.: The subtleties of ultrasound images of an ensemble of cells: simulation from regular and more random distributions of scatterers, 329
Huskova, B., see Hrazdira, I.
Hutchison, K. J.: Doppler ultrasound spectral shape downstream of significant arterial stenosis *in vivo*, 447

Hydrocephalus
monitoring intracranial dynamics by transcranial Doppler—a new Doppler index: trans systolic time (Hanlo), 613

Hydroethidine
flow cytometric analysis of cell suspensions exposed to shock waves in the presence of the radical sensitive dye Hydroethidine (Endl), 569

Hydrogen peroxide
comet assay reveals DNA strand breaks induced by ultrasonic cavitation *in vitro* (Miller), 841
flow cytometric analysis of cell suspensions exposed to shock waves in the presence of the radical sensitive dye Hydroethidine (Endl), 569
ultrasound contrast agents nucleate inertial cavitation *in vitro* (Miller), 1059

Hydrophone
damage to red blood cells induced by acoustic cavitation (Daniels), 105
importance of the implosion of ESWL-induced cavitation bubbles (Delacretaz), 97
influence of water temperature on pressure pulses generated by an electromagnetic type lithotripter (Augat), 89
the cavitation threshold of human tissue exposed to 0.2-MHz pulsed ultrasound: preliminary measurements based on a study of clinical lithotripsy (Coleman), 405
the performance of different pressure pulse generators for extracorporeal lithotripsy: a comparison based on commercial lithotripters for kidney stones (Buizza), 259

Hyperplasia
ultrasound focal beam surgery (ter Haar), 1089

Hypertension
assessment of fetal left cardiac isovolumic relaxation time in appropriate and small-for-gestational-age fetuses (Tsyvian), 739
computer analysis of the early diastolic notch in Doppler sonograms of the uterine arteries (Loupas), 1001

Hyperthermia (see also thermal effects)
ultrasonic heating of the brain of the fetal sheep *in utero* (Duggan), 553
ultrasound focal beam surgery (ter Haar), 1089
ultrasound-guided microwave thermotherapy on a VX-2 carcinoma implanted in rabbit kidney (Kigure), 649

Hypoxia
assessment of the fetal PO_2 changes by cerebral and umbilical Doppler on lamb fetuses during acute hypoxia (Arbeille), 861

I

IGF (insulin-like growth factors)
hematologic and growth-related effects of frequent prenatal ultrasound exposure in the long-tailed macaque (*macaca fascicularis*) (Tarantal), 1073

Iliac arteries
assessment of regional vascular distensibility in diseased iliofemoral arteries by intravascular ultrasound (The), 17

Ilijas, M., see Kupesic, S.

Iliofemoral artery
assessment of regional vascular distensibility in diseased iliofemoral arteries by intravascular ultrasound (The), 17

Image analysis
colour Doppler image analysis for tissue vascularity and perfusion: a preliminary clinical evaluation (Hirsch), 1107
segmentation and analysis of colour Doppler images of tumour vasculature (Bell), 635

Image processing
characterization of ultrasonic B-scans using non-Rayleigh statistics (Molthen), 161
discrimination of intravascular lumen and dissections in single intravascular ultrasound images using subtraction, conventional averaging and saline flush (Pasterkamp), 149
intravascular ultrasound image subtraction: a contrast enhancing technique to facilitate automatic three-dimensional visualization of the arterial lumen (Pasterkamp), 913
registration of three-dimensional compound ultrasound scans of the breast for refraction and motion correction (Moskalik), 769
the subtleties of ultrasound images of an ensemble of cells: simulation from regular and more random distributions of scatterers (Hunt), 329
ultrasonic three-dimensional reconstruction of the heart (Salustri), 281 (Review)
volumetric blood flow measurement by simultaneous Doppler signal and B-mode image processing: a feasibility study (Willink), 481

Imaging
a 40–100 MHz B-scan ultrasound backscatter microscope for skin imaging (Turnbull), 79
registration of three-dimensional compound ultrasound scans of the breast for refraction and motion correction (Moskalik), 769
volumetric blood flow measurement by simultaneous Doppler signal and B-mode image processing: a feasibility study (Willink), 481

Imanaka, M., see Nakai, Y.
Imaoka, T., see Tanaka, S.

In situ *exposimetry*
in situ human obstetrical ultrasound exposimetry: estimates of derating factors for each of three different tissue models (Siddiqi), 379

In utero *exposimetry*
in situ human obstetrical ultrasound exposimetry: estimates of derating factors for each of three different tissue models (Siddiqi), 379

In utero *irradiation*
the effect of ultrasound exposure *in utero* on the development of the fetal mouse testis: adult consequences (Carnes), 1247

In vitro *irradiation*
acoustic energy determines haemoglobin release from erythrocytes by extracorporeal shock waves *in vitro* (Delius), 707
damage to red blood cells induced by acoustic cavitation (Daniels), 105
Doppler velocity ratio measurements evaluated in a phantom model of multiple arterial disease (Allard), 471
effect of therapeutic ultrasound on endochondral ossification (Wiltink), 121
effect of ultrasound on DNA synthesis in tumor cells (Forytková), 585
effects of piezoelectric lithotripsy on human DNA (Bird), 399
effects of ultrasound on agglutination and aggregation of human erythrocytes *in vitro* (Pohl), 711
flow cytometric analysis of cell suspensions exposed to shock waves in the presence of the radical sensitive dye Hydroethidine (Endl), 569
glycoprotein and ganglioside changes in human trophoblasts after exposure to pulsed Doppler ultrasound (Heffer-Lauc), 579
macroscopic ESWL-induced cavitation: *in vitro* studies (Pittomvils), 393
physical factors involved in stress-wave-induced cell injury: the effect of stress gradient (Doukas), 961
pro- and antifibrinolytic effects of ultrasound on streptokinase-induced thrombolysis (Nilsson), 833
roles of hematocrit and fibrinogen in red cell aggregation determined by ultrasonic scattering properties (Kitamura), 827
temperature rise generated by diagnostic ultrasound in a transcranial phantom (Wu), 561
ultrasound accelerates transport of recombinant tissue plasminogen activator into clots (Francis), 419
ultrasound backscatter at 30 MHz from human blood: influence of rouleau size affected by blood modification and shear rate (van der Heiden), 817
ultrasound contrast agents nucleate inertial cavitation *in vitro* (Miller), 1059
ultrasound focal beam surgery (ter Haar), 1089

In vivo *irradiation*
a novel ultrasonic technique for differentiating cysts from solid lesions: preliminary results in the breast (Nightingale), 745
acoustic generation of intra-arterial contrast boluses (Ivey), 757
biological effects of shock waves: *in vivo* effect of high energy pulses on rabbit bone (Delius), 1219
hematologic and growth-related effects of frequent prenatal ultrasound exposure in the long-tailed macaque (*macaca fascicularis*) (Tarantal), 1073
histologic effects of high intensity pulsed ultrasound exposure with subharmonic emission in rabbit brain *in vivo* (Vykhodtseva), 969
prenatal application of diagnostic ultrasound in mice (Hrazdira), 427 (Letter)
the cavitation threshold of human tissue exposed to 0.2-MHz pulsed ultrasound: preliminary measurements based on a study of clinical lithotripsy (Coleman), 405
the effects of successive high-energy shock-wave tumor administration on tumor blood flow (Cornel), 243

thresholds for hemorrhages in mouse skin and intestine induced by lithotripter shock waves (Miller), 249
thresholds for intestinal hemorrhage in mice exposed to a piezoelectric lithotripter (Dalecki), 1239
ultrasonic heating of the brain of the fetal sheep *in utero* (Duggan), 553
ultrasound and microbubbles: their generation, detection and potential utilization in tissue and organ therapy—experimental (Fry), 1227
ultrasound focal beam surgery (ter Haar), 1089
venous thrombosis generation by means of high-intensity focused ultrasound (Delon-Martin), 113

Inertial cavitation
ultrasound contrast agents nucleate inertial cavitation *in vitro* (Miller), 1059

Injections, ethanol
echogenicity of experimental liver ethanol injections (Vehmas), 1137

Insana, M. F., Wood, J. G., Hall, T. J., Cox G. G. and Harrison, L. A.: effects of endothelin-1 on renal microvasculature measured using quantitative ultrasound, 1143

Integrated backscatter
a study of the relationship between mechanical and ultrasonic properties of dystrophic and normal skeletal muscle (Hete), 343
effects of endothelin-1 on renal microvasculature measured using quantitative ultrasound (Insana), 1143
ultrasonic tissue characterization of end-stage dilated cardiomyopathy (Davison), 853
ultrasound backscatter at 30 MHz from human blood: influence of rouleau size affected by blood modification and shear rate (van der Heiden), 817
validation of transthoracic myocardial ultrasonic tissue characterization: comparison of transthoracic and open-chest measurements of integrated backscatter (Naito), 33
when can Doppler be used in place of integrated backscatter as a measure of scattered ultrasound intensity? (Schwarz), 231

Intestinal hemorrhage
intestinal hemorrhage from exposure to pulsed ultrasound (Dalecki), 1067
thresholds for intestinal hemorrhage in mice exposed to a piezoelectric lithotripter (Dalecki), 1239

Intracranial pressure
monitoring intracranial dynamics by transcranial Doppler—a new Doppler index: trans systolic time (Hanlo), 613

Intravascular Doppler catheter
effects of nonuniform insonation by catheter-tipped Doppler transducers on velocity estimation (Moraes), 779

Intravascular ultrasound
assessment of regional vascular distensibility in diseased iliofemoral arteries by intravascular ultrasound (The), 17
discrimination of intravascular lumen and dissections in single intravascular ultrasound images using subtraction, conventional averaging and saline flush (Pasterkamp), 149

effects of nonuniform insonation by catheter-tipped Doppler transducers on velocity estimation (Moraes), 779
intravascular ultrasound image subtraction: a contrast enhancing technique to facilitate automatic three-dimensional visualization of the arterial lumen (Pasterkamp), 913
ultrasound backscatter at 30 MHz from human blood: influence of rouleau size affected by blood modification and shear rate (van der Heiden), 817

Intrinsic spectral broadening
correction of intrinsic spectral broadening errors in Doppler peak velocity measurements made with phased sector and linear array transducers (Winkler), 1029

Irradiation data
comparison of ultrasound irradiation of pregnant mice with other bioeffects data (Fry), 430

IUGR (intrauterine growth retardation)
assessment of fetal left cardiac isovolumic relaxation time in appropriate and small-for-gestational-age fetuses (Tsyvian), 739
computer analysis of the early diastolic notch in Doppler sonograms of the uterine arteries (Loupas), 1001

Ivey, J. A., Gardner, E. A., Fowlkes, J. B., Rubin, J. M. and Carson, P. L.: acoustic generation of intra-arterial contrast boluses, 757
Iyer, V., see Smielewski, P.

J

Jacobs, N., see Fatkin, D.
Jago, J. R.: exposure criteria for medical diagnostic ultrasound: I. criteria based on thermal mechanisms, 425 (Book Review)
Jago, J. R., Henderson, J., Whittingham, T. A. and Willson, K.: how reliable are manufacturer's reported acoustic output data?, 135
Jago, J. R., see Henderson, J.
Jenkins, W. K., see Chen, E. J.
Jensen, H. M., see Burke, T. M.

Jets
a model based on dimensional analysis for noninvasive quantification of valvular regurgitation under confined and impinging conditions: *in vitro* pulsatile flow validation (Burleson), 899
atrial inflow can alter regurgitant jet size: *in vitro* studies (Grimes), 459

Johnson, A. G., see Bird, N. C.
Jones, H. W., see Fleischer, A. C.
Justin, J., see Kitamura, H.

K

Kadi, A. P., see Phillips, P. J.
van Kaick, G., see Fein, M.
Kale S. G., see Hirsch, W.
Kalisz, A., see Kitamura, H.
Kamada, T., see Naito, J.
Kaps, M., Seidel, G. and Berg, J.: is there a hemispheric side preference of cardiac valvular emboli?, 753

Kellnerova, R., see Hrazdira, I.
Kepple, D.M., see Fleischer, A.C.

Keratin
ultrasonic propagation properties of excised human skin (Moran), 1177

Kerr, A. T., see Hunt, J. W.
Keunen, R. W. M., see Hanlo, P. W.

Kidney
a Schlieren study of the interaction between a lithotripter shock wave and a simulated kidney stone (Carnell), 721
effects of endothelin-1 on renal microvasculature measured using quantitative ultrasound (Insana), 1143
elasticity imaging for early detection of renal pathology (Emelianov), 871
electronic beam steering of shock waves (Cathignol), 365
in vivo comparison of 3D ultrasonography and magnetic resonance imaging in volume estimation of human kidneys (Gilja), 25
the performance of different pressure pulse generators for extracorporeal lithotripsy: a comparison based on commercial lithotripters for kidney stones (Buizza), 259
ultrasound focal beam surgery (ter Haar), 1089
ultrasound-guided microwave thermotherapy on a VX-2 carcinoma implanted in rabbit kidney (Kigure), 649

Kidney stone
a Schlieren study of the interaction between a lithotripter shock wave and a simulated kidney stone (Carnell), 721
electronic beam steering of shock waves (Cathignol), 365
the performance of different pressure pulse generators for extracorporeal lithotripsy: a comparison based on commercial lithotripters for kidney stones (Buizza), 259

Kigure, T., Harada, T., Yuri, Y. and Satoh, Y.: ultrasound-guided microwave thermotherapy on a VX-2 carcinoma implanted in rabbit kidney, 649
King, B., see Collins, G. N.
Kitamra, T., see Tanaka, S.
Kitamura, H., Sigel, B., Machi, J., Feleppa, E. J., Sokil-Melgar, J., Kalisz, A. and Justin, J.: roles of hematocrit and fibrinogen in red cell aggregation determined by ultrasonic scattering properties, 827
Kitamura, S., see Tanaka, S.
Kluytmans, M., see Pasterkamp, G.
Kodama, T., see Coleman, A. J.
Kodama, T., see Daniels, S.
Kondo, H., see Naito, J.
Kopf, G. M. A., see Gehmacher, O.
Kornguth, P. J., see Nightingale, K. R.
Kovács, S. J. Jr., see Nudelman, S.
Kristoffersen, K., see Torp, H.
Krone, A., see Becker, G.
de Kroon, M.G.M., see van der Heiden, M.S
Kupesic, S., Kurjak, A., Pasalic, L., Benic, S., Ilijas, M.: the value of transvaginal color Doppler in the assessment of pelvic inflammatory disease, 733
Kurjak, A., see Kupesic, S.
Kynynen, K., see Vykhodtseva, N. I.

L

Lafaut, J. P., see Delacrétaz, G.
Lafaut, J. P., see Pittomvils, G.

Lamb fetus
assessment of the fetal PO_2 changes by cerebral and umbilical Doppler on lamb fetuses during acute hypoxia (Arbeille), 861

Länne, T., see Hansen, F.

Laser Doppler
a numerical and experimental investigation of the flow acceleration region proximal to an orifice (Anayiotos), 501

Latin, V., see Heffer-Lauc, M.
Lauc, G., see Heffer-Lauc, M.

Lectins
glycoprotein and ganglioside changes in human trophoblasts after exposure to pulsed Doppler ultrasound (Heffer-Lauc), 579

Lee, S., see Doukas, A. G.
Lee, S., see Francis, C. W.

Lesion
ultrasound focal beam surgery (ter Haar), 1089

Levine, R. A., see Burleson, A. C.
Levine, R. A., see Grimes, R. Y.

Levovist
effectiveness of galactose-based intravenous contrast medium on color Doppler sonography of deeply located hepatocellular carcinoma (Tanaka), 157

Li, W., see The, S. H. K.
Liberman, F. Z., see Harrison, G. H.
Liggins, G. C., see Duggan, P. M.
Lindner, A., see Becker, G.
Lindström, K., see Eriksson, R.

Lithotripsy
a Schlieren study of the interaction between a lithotripter shock wave and a simulated kidney stone (Carnell), 721
effects of piezoelectric lithotripsy on human DNA (Bird), 399
electronic beam steering of shock waves (Cathignol), 365
flow cytometric analysis of cell suspensions exposed to shock waves in the presence of the radical sensitive dye Hydroethidine (Endl), 569
importance of the implosion of ESWL-induced cavitation bubbles (Delacretaz), 97
influence of water temperature on pressure pulses generated by an electromagnetic type lithotripter (Augat), 89
macroscopic ESWL-induced cavitation: *in vitro* studies (Pittomvils), 393
the cavitation threshold of human tissue exposed to 0.2-MHz pulsed ultrasound: preliminary measurements based on a study of clinical lithotripsy (Coleman), 405
the performance of different pressure pulse generators for extracorporeal

lithotripsy: a comparison based on commercial lithotripters for kidney stones (Buizza), 259
thresholds for hemorrhages in mouse skin and intestine induced by lithotripter shock waves (Miller), 249
thresholds for intestinal hemorrhage in mice exposed to a piezoelectric lithotripter (Dalecki), 1239

Litter size
the effect of ultrasound exposure *in utero* on the development of the fetal mouse testis: adult consequences (Carnes), 1247

Liu, J.-B., see Forsberg, F.

Liver
echogenicity of experimental liver ethanol injections (Vehmas), 1137
effectiveness of galactose-based intravenous contrast medium on color Doppler sonography of deeply located hepatocellular carcinoma (Tanaka), 157
ultrasound focal beam surgery (ter Haar), 1089

Liver neoplasm
echogenicity of experimental liver ethanol injections (Vehmas), 1137
effectiveness of galactose-based intravenous contrast medium on color Doppler sonography of deeply located hepatocellular carcinoma (Tanaka), 157

Lobules
preliminary investigation of ultrasound scattering analysis to identify women at risk for later invasive cancer. I: motivation and experimental technique for characterization of isolated breast tissue lobules (Burke), 295

Local recurrence
preoperative and postoperative follow-up in high-grade gliomas: comparison of transcranial color-coded real-time sonography and computed tomography findings (Becker), 1123

Locatelli, A., see Arbeille, P.
Locatelli, A., see Arbeille, Ph.
Lopath, P. D., see Smith, S. W.
Loupas, T., Ellwood, D. A., Gill, R. W., Bruce, S. and Fay, R. A.: computer analysis of the early diastolic notch in Doppler sonograms of the uterine arteries, 1001
Loupas, T., see Fatkin, D.
Lubinski, M. A., see Emelianov, S. Y.

Lumen
discrimination of intravascular lumen and dissections in single intravascular ultrasound images using subtraction, conventional averaging and saline flush (Pasterkamp), 149
intravascular ultrasound image subtraction: a contrast enhancing technique to facilitate automatic three-dimensional visualization of the arterial lumen (Pasterkamp), 913

Lumen dimensions
assessment of regional vascular distensibility in diseased iliofemoral arteries by intravascular ultrasound (The), 17

diameter and compliance in the human common carotid artery—variations with age and sex (Hansen), 1
volumetric blood flow measurement by simultaneous Doppler signal and B-mode image processing: a feasibility study (Willink), 481

Lung abscess
ultrasound imaging of pneumonia (Gehmacher), 1119

Lung effects
microscopic lung alterations and reduction of respiration rate in insonated anesthetized swine (Harrison), 981

M

M mode
assessment of fetal left cardiac isovolumic relaxation time in appropriate and small-for-gestational-age fetuses (Tsyvian), 739

Machi, J., see Kitamura, H.
Madsen, E. L., see Holden, J. E.

Magnetic resonance imaging (MRI)
in vivo comparison of 3D ultrasonography and magnetic resonance imaging in volume estimation of human kidneys (Gilja), 25

Malkin, K., see Tsyvian, P.
Manfredi, C., see Fort, A.
Mangell, P., see Hansen, F.
Mano, T., see Naito, J.
Manson, A. L., see Nudelman, S.
Masuyama, T., see Naito, J.
Matre, K., see Gilja, O. H.
Maulik, D., see Arbeille, P.

Maximum frequency estimation
adaptive SVD-based AR model order determination for time-frequency analysis of Doppler ultrasound signals (Fort), 793

Maxwell model
a survey of the acoustic outputs of diagnostic ultrasound equipment in current clinical use (Henderson), 699

McArdle, A., Newhouse, V. L. and Beach, K. W.: demonstration of three-dimensional vector flow estimation using bandwidth and two transducers on a flow phantom, 679
McAuliffe, D. J., see Doukas, A. G.
McCready, V. R., see Hirsch, W.
McDermott, B. A., see Nightingale, K. R.

Mean frequency estimation
bias in mean frequency estimation of Doppler signals due to wall clutter filters (Tysoe), 671

Mean velocity estimation
the effect of echo suppression on the mean velocity estimation range of the RF cross-correlation model estimator (Brands), 945

Mechanical effects
ultrasound focal beam surgery (ter Haar), 1089

Mechanical index
thresholds for hemorrhages in mouse skin and intestine induced by lithotripter shock waves (Miller), 249

Melanoma
a 40–100 MHz B-scan ultrasound backscatter microscope for skin imaging (Turnbull), 79

Membrane permeability
physical factors involved in stress-wave-induced cell injury: the effect of stress gradient (Doukas), 961

Metatarse
effect of therapeutic ultrasound on endochondral ossification (Wiltink), 121

Meyer, C. R., see Moskalik, A.
Meyer, R. A., see Siddiqi, T. A.

Mice
comparison of ultrasound irradiation of pregnant mice with other bioeffects data (Fry), 430 (Letter)
intestinal hemorrhage from exposure to pulsed ultrasound (Dalecki), 1067
prenatal application of diagnostic ultrasound in mice (Hrazdira), 427 (Letter)
the effect of ultrasound exposure *in utero* on the development of the fetal mouse testis: adult consequences (Carnes), 1247
thresholds for intestinal hemorrhage in mice exposed to a piezoelectric lithotripter (Dalecki), 1239

Micro-architecture
preliminary investigation of ultrasound scattering analysis to identify women at risk for later invasive cancer. I: motivation and experimental technique for characterization of isolated breast tissue lobules (Burke), 295
preliminary investigation of ultrasound scattering analysis to identify women at risk for later invasive cancer. II: extraction of dominant scattering angle-dependent trends from excised breast tissue (Burke), 305

Microbubbles
echogenicity of experimental liver ethanol injections (Vehmas), 1137
ultrasound and microbubbles: their generation, detection and potential utilization in tissue and organ therapy—experimental (Fry), 1227

Microscope
a 40–100 MHz B-scan ultrasound backscatter microscope for skin imaging (Turnbull), 79

Microwave
ultrasound-guided microwave thermotherapy on a VX-2 carcinoma implanted in rabbit kidney (Kigure), 649

Middle cerebral artery
computerised transient hyperaemic response test—a method for the assessment of cerebral autoregulation (Smielewski), 599

Miller, D. L. and Thomas, R. M.: thresholds for hemorrhages in mouse skin and intestine induced by lithotripter shock waves, 249
Miller, D. L. and Thomas, R. M.: ultrasound contrast agents nucleate inertial cavitation *in vitro*, 1059
Miller, D. L., Thomas, R. M. and Buschbom, R. L.: comet assay reveals DNA strand breaks induced by ultrasonic cavitation *in vitro*, 841
Miller, J. G., see Davison, G.
Millner, R., see Pohl, E. E.

Minimally invasive surgery
histologic effects of high intensity pulsed ultrasound exposure with subharmonic emission in rabbit brain *in vivo* (Vykhodtseva), 969

Miodovnik, M., see Siddiqi, T. A.

Mitral regurgitation
atrial inflow can alter regurgitant jet size: *in vitro* studies (Grimes), 459

Modelling
a model based on dimensional analysis for noninvasive quantification of valvular regurgitation under confined and impinging conditions: *in vitro* pulsatile flow validation (Burleson), 899
a numerical and experimental investigation of the flow acceleration region proximal to an orifice (Anayiotos), 501
a study of the relationship between mechanical and ultrasonic properties of dystrophic and normal skeletal muscle (Hete), 343
a wall-less vessel phantom for Doppler ultrasound studies (Rickey), 1163
adaptive SVD-based AR model order determination for time-frequency analysis of Doppler ultrasound signals (Fort), 793
cardiac ultrasound phantom using a porcine heart model (Smith), 693
changes in ultrasonic Doppler backscattered power downstream of concentric and eccentric stenoses under pulsatile flow (Cloutier), 59
characterization of ultrasonic B-scans using non-Rayleigh statistics (Molthen), 161
comparison of diastolic filling models and their fit to transmitral Doppler contours (Nudelman), 989
Doppler velocity ratio measurements evaluated in a phantom model of multiple arterial disease (Allard), 471
errors in transrectal ultrasonic planimetry of the prostate: computer simulation of volumetric errors applied to a screening population (Bangma), 11
fundamental mechanical limitations on the visualization of elasticity contrast in elastography (Ponnekanti), 533
in situ human obstetrical ultrasound exposimetry: estimates of derating factors for each of three different tissue models (Siddiqi), 379
monitoring intracranial dynamics by transcranial Doppler—a new Doppler index: trans systolic time (Hanlo), 613
nonlinear behavior of a liquid containing uniform bubbles: comparison between theory and experiments (Wu), 545
parameter mapping for the detection of disturbed blood flow (Ferrara), 517
quantification of intravenous contrast-enhanced Doppler power spectrum in the rabbit carotid artery (Frush), 41
quantitative investigation of *in vitro* flow using three-dimensional colour Doppler ultrasound (Guo), 807
roles of hematocrit and fibrinogen in red cell aggregation determined by ultrasonic scattering properties (Kitamura), 827

the butterfly search technique for estimation of blood velocity (Alam), 657
time-domain ultrasonic contrast blood flowmetry (Shung), 71
ultrasonic heating of the brain of the fetal sheep *in utero* (Duggan), 553
ultrasonic tissue characterization of end-stage dilated cardiomyopathy (Davison), 853
volumetric blood flow calculation using a narrow ultrasound beam (Willink), 203
when can Doppler be used in place of integrated backscatter as a measure of scattered ultrasound intensity? (Schwarz), 231

Molthen, R. C., Shankar, P. M. and Reid, J. M.: characterization of ultrasonic B-scans using non-Rayleigh statistics, 161

Monkey
hematologic and growth-related effects of frequent prenatal ultrasound exposure in the long-tailed macaque (macaca fascicularis) (Tarantal), 1073

Moraes, R. and Evans D. H.: effects of nonuniform insonation by catheter-tipped Doppler transducers on velocity estimation, 779
Moran, C. M., Bush, N. L. and Bamber, J. C.: ultrasonic propagation properties of excised human skin, 1177
Moreau, M., see Guo, Z.
Mornstein, V., see Forytková, L.
Moskalik, A., Carson, P. L., Meyer, C. R., Fowlkes, J. B., Rubin, J. M. and Roubidoux, M. A.: registration of three-dimensional compound ultrasound scans of the breast for refraction and motion correction, 769

Motion
registration of three-dimensional compound ultrasound scans of the breast for refraction and motion correction (Moskalik), 769
ultrasound tissue displacement imaging with application to breast cancer (Chen), 1153

Motion correction
registration of three-dimensional compound ultrasound scans of the breast for refraction and motion correction (Moskalik), 769

Moulaert, A.-F. S. R., see Pasterkamp, G.

MRI, see magnetic resonance imaging

Müller, W. E. G., see Heffer-Lauc, M.

Multifrequency Doppler
blood perfusion measurement with multifrequency Doppler ultrasound (Eriksson), 49

Murakami, K., see Naito, J.

Muscle
ultrasound focal beam surgery (ter Haar), 1089

Muscular dystrophy
a study of the relationship between mechanical and ultrasonic properties of dystrophic and normal skeletal muscle (Hete), 343

Mykers, J. G., see Anayiotos, A. S.

Myocardium
validation of transthoracic myocardial ultrasonic tissue characterization: comparison of transthoracic and open-chest measurements of integrated backscatter (Naito), 33

N

N'Guyen, T., see Burleson, A.C.
Nachef, S., see Cathignol, D.
Naito, J., Masuyama, T., Mano, T., Yamamoto, K., Doi, Y., Kondo, H., Hori, M., Shiba, A., Murakami, K., Shimura, T. and Kamada, T.: validation of transthoracic myocardial ultrasonic tissue characterization: comparison of transthoracic and open-chest measurements of integrated backscatter, 33
Nakai, Y., Imanaka, M., Nishio, J. and Ogita, S.: umbilical cord venous pulsation in normal fetuses and its incidence after 13 weeks of gestation, 443
Nanda, N. C., see Anayiotos, A. S.
Nanda, N. C., see Fan, P.

Narrow vessels
improved blood velocity estimation using the maximum Doppler frequency (Tortoli), 527

Newhouse, V. L., see McArdle, A.
Newhouse, V. L., see Tortoli, P.
Niemer, A. Q. H. J., see Bangma, C. H.
Nightingale, K. R., Kornguth, P. J., Walker, W. F., McDermott, B. A. and Trahey, G. E.: a novel ultrasonic technique for differentiating cysts from solid lesions: preliminary results in the breast, 745
Nijweide, P. J., see Wiltink, A.
Nilsson, A.-M., Odselius, R., Roijer, A. and Olsson, S. B.: pro- and antifibrinolytic effects of ultrasound on streptokinase-induced thrombolysis, 833
Nishio, J., see Nakai, Y.

NMR spectroscopy
the effects of successive high-energy shock-wave tumor administration on tumor blood flow (Cornel), 243

Non-Rayleigh statistics
characterization of ultrasonic B-scans using non-Rayleigh statistics (Molthen), 161

Nonaxial flow
experimental velocity profiles and volumetric flow via two-dimensional speckle tracking (Bohs), 885

Nonlinear effects
venous thrombosis generation by means of high-intensity focused ultrasound (Delon-Martin), 113

Nonlinearity
nonlinear behaviour of a liquid containing uniform bubbles: comparison between theory and experiments (Wu), 545

Nudelman, S., Manson, A. L., Hall, A. F. and Kovács, S. J., Jr.: comparison of diastolic filling models and their fit to transmitral Doppler contours, 989

Nyarko, S. J., see Grimes, R. Y.

Nyquist
velocity matched spectrum analysis: a new method for suppressing velocity ambiguity in pulsed-wave Doppler (Torp), 937

O

O'Brien, W. D. Jr., see Chen, E. J.
O'Brien, W. D. Jr., see Siddiqi, T. A.
O'Brien, W. D. Jr., see Tarantal, A. F.
O'Donnell, M., see Emelianov, S. Y.

Observer variation
reproducibility and observer variability of transrectal ultrasound measurements of prostatic volume (Collins), 1101

Obstetrics
assessment of fetal left cardiac isovolumic relaxation time in appropriate and small-for-gestational-age fetuses (Tsyvian), 739
in situ human obstetrical ultrasound exposimetry: estimates of derating factors for each of three different tissue models (Siddiqi), 379
umbilical cord venous pulsation in normal fetuses and its incidence after 13 weeks of gestation (Nakai), 443

Odegaard, S., see Gilja, O. H.
Odselius, R., see Nilsson, A.-M.
Ogita, S., see Nakai, Y.
Olsson, S. B., see Nilsson, A.-M.

Oncology
ultrasound focal beam surgery (ter Haar), 1089

Oosterbaan, W. A., see Wiltink, A.
Oosterhof, G. O. N., see Cornel, E. B.
Ooura, Y., see Tanaka, S.
Ophir, J., see Ponnekanti, H.

Ophthalmology
ultrasound focal beam surgery (ter Haar), 1089

Oscillating bubbles
nonlinear behavior of a liquid containing uniform bubbles: comparison between theory and experiments (Wu), 545

Ostromogilsky, M., see Ferrara, K. W.

Ovarian artery
reproducibility of Doppler measurements of blood flow velocity in the uterine and ovarian arteries in premenopausal women (Sladkevicius), 313
Öztürk Turhan, N., see Dilmen, G.
Öztürk, M., see Dilmen, G.

P

Pallister, J.E., see Adler, R.S.
Parker, K. J., see Alam, S. K.
Pasalic, L., see Kupesic, S.

Pasterkamp, G., Borst, C., Moulaert, A.-F. S. R., Bouma, C. J., van Dijk, D., Kluytmans, M. and ter Haar Romeny, B. M.: intravascular ultrasound image subtraction: a contrast enhancing technique to facilitate automatic three-dimensional visualization of the arterial lumen, 913
Pasterkamp, G., van der Heiden, M. S., Post, M. J., Borst, C., Gussenhoven, E. J., Pieterman, H., van Urk, H. and Bom, N.: discrimination of intravascular lumen and dissections in single intravascular ultrasound images using subtraction, conventional averaging and saline flush, 149
Peery, C. V., see Fleischer, A. C.

Percutaneous ethanol treatment
ultrasound guided percutaneous ethanol treatment of hepatic neoplasms: a therapeutic alternative in the nineties (Bastid), 129 (CN)

Percutaneous procedure
ultrasound-guided microwave thermotherapy on a VX-2 carcinoma implanted in rabbit kidney (Kigure), 649
ultrasound guided percutaneous ethanol treatment of hepatic neoplasms: a therapeutic alternative in the nineties (Bastid), 129 (CN)

Perflubron emulsion
quantification of intravenous contrast-enhanced Doppler power spectrum in the rabbit carotid artery (Frush), 41

Perfusion
acoustic generation of intra-arterial contrast boluses (Ivey), 757
background subtraction from time-intensity curves in videodensitometry: a pitfall in flow assessment using contrast echocardiography (Bos), 1211
blood perfusion measurement with multifrequency Doppler ultrasound (Eriksson), 49
colour Doppler image analysis for tissue vascularity and perfusion: a preliminary clinical evaluation (Hirsch), 1107
effects of endothelin-1 on renal microvasculature measured using quantitative ultrasound (Insana), 1143
quantification of color Doppler for the evaluation of tissue vascularization (Fein), 1013

Perfusion phantom
background subtraction from time-intensity curves in videodensitometry: a pitfall in flow assessment using contrast echocardiography (Bos), 1211

Perry, G. J., see Anayiotos, A. S.
Persson, H. W., see Eriksson, R.

Petechia
thresholds for hemorrhages in mouse skin and intestine induced by lithotripter shock waves (Miller), 248

Peters, R. J. A., see Hanlo, P. W.

Phantom
a model based on dimensional analysis for noninvasive quantification of valvular regurgitation under confined and impinging conditions: *in vitro* pulsatile flow validation (Burleson), 899
a noninvasive method to estimate wall shear rate using ultrasound (Brands), 171

a numerical and experimental investigation of the flow acceleration region proximal to an orifice (Anayiotos), 501
atrial inflow can alter regurgitant jet size: *in vitro* studies (Grimes), 459
background subtraction from time-intensity curves in videodensitometry: a pitfall in flow assessment using contrast echocardiography (Bos), 1211
blood perfusion measurement with multifrequency Doppler ultrasound (Eriksson), 49
cardiac ultrasound phantom using a porcine heart model (Smith), 693
changes in ultrasonic Doppler backscattered power downstream of concentric and eccentric stenoses under pulsatile flow (Cloutier), 59
correction of intrinsic spectral broadening errors in Doppler peak velocity measurements made with phased sector and linear array transducers (Winkler), 1029
demonstration of three-dimensional vector flow estimation using bandwidth and two transducers on a flow phantom (McArdle), 679
Doppler velocity ratio measurements evaluated in a phantom model of multiple arterial disease (Allard), 471
effectiveness of galactose-based intravenous contrast medium on color Doppler sonography of deeply located hepatocellular carcinoma (Tanaka), 157
effects of stenosis on transit-time ultrasound measurements of blood flow (Gordon), 623
elasticity imaging for early detection of renal pathology (Emelianov), 871
fundamental mechanical limitations on the visualization of elasticity contrast in elastography (Ponnekanti), 533
parameter mapping for the detection of disturbed blood flow (Ferrara), 517
quantitative investigation of *in vitro* flow using three-dimensional colour Doppler ultrasound (Guo), 807
rapid volume flow rate estimation using transverse colour Doppler imaging (Picot), 1199
temperature rise generated by diagnostic ultrasound in a transcranial phantom (Wu), 561
the butterfly search technique for estimation of blood velocity (Alam), 657
time-domain ultrasonic contrast blood flowmetry (Shung), 71
transesophageal color Doppler evaluation of obstructive lesions using the new "Quasar" technology (Fan), 1021
ultrasonic estimation of tissue perfusion: a stochastic approach (Adler), 493
when can Doppler be used in place of integrated backscatter as a measure of scattered ultrasound intensity? (Schwarz), 231

Phillips, P. J., Kadi, A. P. and von Ramm, O. T.: feasibility study for a two-dimensional diagnostic ultrasound velocity mapping system, 217

Photoacoustics
physical factors involved in stress-wave-induced cell injury: the effect of stress gradient (Doukas), 961

PI (pulsatility index)
monitoring intracranial dynamics by transcranial Doppler—a new Doppler index: trans systolic time (Hanlo), 613
serial assessment of adnexal masses with transvaginal color Doppler sonography (Fleischer), 435

Pickard, J., see Smielewski, P.
Picot, P. A., Fruitman, M., Rankin, R. N. and Fenster, A.: rapid volume flow rate estimation using transverse colour Doppler imaging, 1199

Picot, P. A., see Guo, Z.
Picot, P. A., see Rickey, D. W.
Piechnik, S., see Smielewski, P.
Piek, J. J., see Bos, L. J.
Pieterman, H., see Pasterkamp, G.
Pieterman, H., see The, S. H. K.

Pig
cardiac ultrasound phantom using a porcine heart model (Smith), 693

Pittomvils, G., Lafaut, J. P., Vandeursen, H., De Ridder, D., Baert, L. and Boving, R.: macroscopic ESWL-induced cavitation: *in vitro* studies, 393
Pittomvils, G., see Delacrétaz, G.

Planimetry
errors in transrectal ultrasonic planimetry of the prostate: computer simulation of volumetric errors applied to a screening population (Bangma), 11

Plethysmography
colour Doppler image analysis for tissue vascularity and perfusion: a preliminary clinical evaluation (Hirsch), 1107

Pleural effusion
ultrasound imaging of pneumonia (Gehmacher), 1119

Pneumonia
ultrasound imaging of pneumonia (Gehmacher), 1119

Pohl, E. E., Rosenfeld, E. H., Pohl, P. and Millner, R.: effects of ultrasound on agglutination and aggregation of human erythrocytes *in vitro*, 711
Pohl, P., see Pohl, E. E.

Poisson's ratio
fundamental mechanical limitations on the visualization of elasticity contrast in elastography (Ponnekanti), 533

Polyether block amide
acoustic properties of some biocompatible polymers at body temperature (Guess), 273

Polymer
acoustic properties of some biocompatible polymers at body temperature (Guess), 273

Polyurethane
acoustic properties of some biocompatible polymers at body temperature (Guess), 273

Ponnekanti, H., Ophir, J., Huang, Y. and Céspedes, I.: fundamental mechanical limitations on the visualization of elasticity contrast in elastography, 533
Post, M. J., see Pasterkamp, G.

Postpartum death
the effect of ultrasound exposure *in utero* on the development of the fetal mouse testis: adult consequences (Carnes), 1247

Power mode Doppler
changes in ultrasonic Doppler backscattered power downstream of concentric and eccentric stenoses under pulsatile flow (Cloutier), 59
ultrasonic estimation of tissue perfusion: a stochastic approach (Adler), 493

Power spectrum
quantification of intravenous contrast-enhanced Doppler power spectrum in the rabbit carotid artery (Frush), 41

Pregnancy induced hypertension
assessment of fetal left cardiac isovolumic relaxation time in appropriate and small-for-gestational-age fetuses (Tsyvian), 739

Premenopausal flow
reproducibility of Doppler measurements of blood flow velocity in the uterine and ovarian arteries in premenopausal women (Sladkevicius), 313

Prenatal exposure
hematologic and growth-related effects of frequent prenatal ultrasound exposure in the long-tailed macaque (macaca fascicularis) (Tarantal), 1073

Pressure distribution
electronic beam steering of shock waves (Cathignol), 365
influence of water temperature on pressure pulses generated by an electromagnetic type lithotripter (Augat), 89
the performance of different pressure pulse generators for extracorporeal lithotripsy: a comparison based on commercial lithotripters for kidney stones (Buizza), 259

Pressure measurement
electronic beam steering of shock waves (Cathignol), 365
influence of water temperature on pressure pulses generated by an electromagnetic type lithotripter (Augat), 89
the cavitation threshold of human tissue exposed to 0.2-MHz pulsed ultrasound: preliminary measurements based on a study of clinical lithotripsy (Coleman), 405

Pressure pulse lithotripsy (see ESWL)

Price, D. J., see Daniels, S.

Principal component analysis
preliminary investigation of ultrasound scattering analysis to identify women at risk for later invasive cancer. II: extraction of dominant scattering angle-dependent trends from excised breast tissue (Burke), 305

Propagation
influence of water temperature on pressure pulses generated by an electromagnetic type lithotripter (Augat), 89
ultrasonic propagation properties of excised human skin (Moran), 1177

Prostate
errors in transrectal ultrasonic planimetry of the prostate: computer simulation of volumetric errors applied to a screening population (Bangma), 11
reproducibility and observer variability of transrectal ultrasound measurements of prostatic volume (Collins), 1101

ultrasound and microbubbles: their generation, detection and potential utilization in tissue and organ therapy—experimental (Fry), 1227
ultrasound focal beam surgery (ter Haar), 1089

Prostate volume
errors in transrectal ultrasonic planimetry of the prostate: computer simulation of volumetric errors applied to a screening population: regarding Bangma et al. UMB 21(1):11–16; 1995 (Aarnink), 1083
reproducibility and observer variability of transrectal ultrasound measurements of prostatic volume (Collins), 1101

Prostatic hyperplasia
reproducibility and observer variability of transrectal ultrasound measurements of prostatic volume (Collins), 1101
ultrasound and microbubbles: their generation, detection and potential utilization in tissue and organ therapy—experimental (Fry), 1227
ultrasound focal beam surgery (ter Haar), 1089

Prosthetic heart valve
is there a hemispheric side preference of cardiac valvular emboli? (Kaps), 753

Proximal orifice flow field
a numerical and experimental investigation of the flow acceleration region proximal to an orifice (Anayiotos), 501

Pseudoarthrosis
biological effects of shock waves: *in vivo* effect of high energy pulses on rabbit bone (Delius), 1219

Pulido, G. A., see Grimes, R. Y.

Pulmonary consolidation
ultrasound imaging of pneumonia (Gehmacher), 1119

Pulmonary infarction
ultrasound imaging of pneumonia (Gehmacher), 1119

Pulmonary venous flow
atrial inflow can alter regurgitant jet size: *in vitro* studies (Grimes), 459

Pulsatile flow
changes in ultrasonic Doppler backscattered power downstream of concentric and eccentric stenoses under pulsatile flow (Cloutier), 59
volumetric blood flow calculation using a narrow ultrasound beam (Willink), 203

Pulsatile flow phantom
effects of stenosis on transit-time ultrasound measurements of blood flow (Gordon), 623
transesophageal color Doppler evaluation of obstructive lesions using the new "Quasar" technology (Fan), 1021
volume flow estimation using time domain correlation and ultrasonic flowmetry (Forsberg), 1037

Pulsating bubbles
nonlinear behavior of a liquid containing uniform bubbles: comparison between theory and experiments (Wu), 545

Pulsed Doppler
a noninvasive method to estimate wall shear rate using ultrasound (Brands), 171
assessment of fetal left cardiac isovolumic relaxation time in appropriate and small-for-gestational-age fetuses (Tsyvian), 739
Doppler velocity ratio measurements evaluated in a phantom model of multiple arterial disease (Allard), 471
glycoprotein and ganglioside changes in human trophoblasts after exposure to pulsed Doppler ultrasound (Heffer-Lauc), 579
the butterfly search technique for estimation of blood velocity (Alam), 657
the effect of echo suppression on the mean velocity estimation range of the RF cross-correlation model estimator (Brands), 945
the value of transvaginal color Doppler in the assessment of pelvic inflammatory disease (Kupesic), 733
velocity matched spectrum analysis: a new method for suppressing velocity ambiguity in pulsed-wave Doppler (Torp), 937

Q

Quantification
colour Doppler image analysis for tissue vascularity and perfusion: a preliminary clinical evaluation (Hirsch), 1107
effects of endothelin-1 on renal microvasculature measured using quantitative ultrasound (Insana), 1143
quantification of blood echogenicity: evaluation of a semiquantitative method of grading spontaneous echo contrast (Fatkin), 1191
quantification of color Doppler for the evaluation of tissue vascularization (Fein), 1013
quantification of intravenous contrast-enhanced Doppler power spectrum in the rabbit carotid artery (Frush), 41
quantitative investigation of *in vitro* flow using three-dimensional colour Doppler ultrasound (Guo), 807
when can Doppler be used in place of integrated backscatter as a measure of scattered ultrasound intensity? (Schwarz), 231

Quasar
transesophageal color Doppler evaluation of obstructive lesions using the new "Quasar" technology (Fan), 1021

R

Raab, G. M., see Collins, G. N.

Rabbit
biological effects of shock waves: *in vivo* effect of high energy pulses on rabbit bone (Delius), 1219
elasticity imaging for early detection of renal pathology (Emelianov), 871
histologic effects of high intensity pulsed ultrasound exposure with subharmonic emission in rabbit brain *in vivo* (Vykhodtseva), 969
quantification of intravenous contrast-enhanced Doppler power spectrum in the rabbit carotid artery (Frush), 41

rabbit model of anti-GBM disease elasticity imaging for early detection of renal pathology (Emelianov), 871

Radiation force
a novel ultrasonic technique for differentiating cysts from solid lesions: preliminary results in the breast (Nightingale), 745

Radio frequency (RF)
a noninvasive method to estimate wall shear rate using ultrasound (Brands), 171
a survey of the acoustic outputs of diagnostic ultrasound equipment in current clinical use (Henderson), 699
the effect of echo suppression on the mean velocity estimation range of the RF cross-correlation model estimator (Brands), 945
ultrasonic tissue characterization of end-stage dilated cardiomyopathy (Davison), 853
validation of transthoracic myocardial ultrasonic tissue characterization: comparison of transthoracic and open-chest measurements of integrated backscatter (Naito), 33

Raeman, C. H., see Dalecki, D.
von Ramm, O. T., see Phillips, P. J.
Rankin, R. N., see Picot, P. A.

Real-time volumetric scan
ultrasonic three-dimensional reconstruction of the heart (Salustri), 281 (Review)

Red blood cell aggregation
roles of hematocrit and fibrinogen in red cell aggregation determined by ultrasonic scattering properties (Kitamura), 827
ultrasound backscatter at 30 MHz from human blood: influence of rouleau size affected by blood modification and shear rate (van der Heiden), 817

Red blood cells
acoustic energy determines haemoglobin release from erythrocytes by extracorporeal shock waves *in vitro* (Delius), 707
damage to red blood cells induced by acoustic cavitation (Daniels), 105

Refraction
registration of three-dimensional compound ultrasound scans of the breast for refraction and motion correction (Moskalik), 769
the effect of refraction and assumed speeds of sound in tissue and blood on Doppler ultrasound blood velocity measurements (Christopher), 187

Regression
serial assessment of adnexal masses with transvaginal color Doppler sonography (Fleischer), 435

Regurgitation
a model based on dimensional analysis for noninvasive quantification of valvular regurgitation under confined and impinging conditions: *in vitro* pulsatile flow validation (Burleson), 899
atrial inflow can alter regurgitant jet size: *in vitro* studies (Grimes), 459

Regurgitant flow rate
a model based on dimensional analysis for noninvasive quantification of valvular regurgitation under confined and impinging conditions: *in vitro* pulsatile flow validation (Burleson), 899
atrial inflow can alter regurgitant jet size: *in vitro* studies (Grimes), 459

Reid, J.: special issue in honor of John M. Reid, Vol. 20(7) 1994, 593
Reid, J. M., see Molthen, R. C.

Renal fibrosis
elasticity imaging for early detection of renal pathology (Emelianov), 871

Renal pathology
elasticity imaging for early detection of renal pathology (Emelianov), 871

Renal stones
electronic beam steering of shock waves (Cathignol), 365

Renal tumour
ultrasound-guided microwave thermotherapy on a VX-2 carcinoma implanted in rabbit kidney (Kigure), 649

Reneman, R. S., see Brands, P. J.

Reproducibility
reproducibility and observer variability of transrectal ultrasound measurements of prostatic volume (Collins), 1101
reproducibility of Doppler measurements of blood flow velocity in the uterine and ovarian arteries in premenopausal women (Sladkevicius), 313

Resolution
demonstration of three-dimensional vector flow estimation using bandwidth and two transducers on a flow phantom (McArdle), 679

Resorption
effect of therapeutic ultrasound on endochondral ossification (Wiltink), 121

RF (see also radio frequency)
a noninvasive method to estimate wall shear rate using ultrasound (Brands), 171
a survey of the acoustic outputs of diagnostic ultrasound equipment in current clinical use (Henderson), 699
the effect of echo suppression on the mean velocity estimation range of the RF cross-correlation model estimator (Brands), 945
ultrasonic tissue characterization of end-stage dilated cardiomyopathy (Davison), 853
validation of transthoracic myocardial ultrasonic tissue characterization: comparison of transthoracic and open-chest measurements of integrated backscatter (Naito), 33

RF cross-correlation
a noninvasive method to estimate wall shear rate using ultrasound (Brands), 171
the effect of echo suppression on the mean velocity estimation range of the RF cross-correlation model estimator (Brands), 945

RF data analysis
a noninvasive method to estimate wall shear rate using ultrasound (Brands), 171
the effect of echo suppression on the mean velocity estimation range of the RF cross-correlation model estimator (Brands), 945
ultrasonic tissue characterization of end-stage dilated cardiomyopathy (Davison), 853

RI (resistance index)
assessment of the fetal PO_2 changes by cerebral and umbilical Doppler on lamb fetuses during acute hypoxia (Arbeille), 861
effects of endothelin-1 on renal microvasculature measured using quantitative ultrasound (Insana), 1143
monitoring intracranial dynamics by transcranial Doppler—a new Doppler index: trans systolic time (Hanlo), 613
the value of transvaginal color Doppler in the assessment of pelvic inflammatory disease (Kupesic), 733
umbilical cord venous pulsation in normal fetuses and its incidence after 13 weeks of gestation (Nakai), 443
vascular resistance quantification in high flow resistance areas using the Doppler method (Arbeille), 321

Rickey, D. W., Picot, P. A., Christopher, D. A. and Fenster, A.: a wall-less vessel phantom for Doppler ultrasound studies, 1163
Rickey, D. W., see Guo, Z.
De Ridder, D., see Pittomvils, G.
Rink, K., see Delacrétaz, G.
Rocchi, S., see Fort, A.
Roelandt, J. R. T. C., see Salustri, A.
Roelandt, J. R. T. C., see The, S. H. K.
Roijer, A., see Nilsson, A.-M.
Roosen, K., see Becker, G.
Rosenberg, S., see Ferrara, K. W.
Rosenfeld, E. H., see Pohl, E. E.
Ross, B., see Bird, N. C.
Roubidoux, M. A., see Moskalik, A.

Rouleau
ultrasound backscatter at 30 MHz from human blood: influence of rouleau size affected by blood modification and shear rate (van der Heiden), 817
Rubin, J. M., see Adler, R. S.
Rubin, J. M., see Ivey, J. A.
Rubin, J. M., see Moskalik, A.
Russell, K. M., see Forsberg, F.

S

Safety
a survey of the acoustic outputs of diagnostic ultrasound equipment in current clinical use (Henderson), 699
effect of ultrasound on DNA synthesis in tumor cells (Forytková), 585
glycoprotein and ganglioside changes in human trophoblasts after exposure to pulsed Doppler ultrasound (Heffer-Lauc), 579
hematologic and growth-related effects of frequent prenatal ultrasound exposure in the long-tailed macaque (macaca fascicularis) (Tarantal), 1073

in situ human obstetrical ultrasound exposimetry: estimates of derating factors for each of three different tissue models (Siddiqi), 379
temperature rise generated by diagnostic ultrasound in a transcranial phantom (Wu), 561
ultrasonic heating of the brain of the fetal sheep *in utero* (Duggan), 553

Sahel, J., see Bastid, C.

Saline flush
discrimination of intravascular lumen and dissections in single intravascular ultrasound images using subtraction, conventional averaging and saline flush (Pasterkamp), 149

Salustri, A. and Roelandt, J. R. T. C.: ultrasonic three-dimensional reconstruction of the heart, 281

Sample volume
demonstration of three-dimensional vector flow estimation using bandwidth and two transducers on a flow phantom (McArdle), 679
effects of nonuniform insonation by catheter-tipped Doppler transducers on velocity estimation (Moraes), 779

Sanghvi, N. T., see Fry, F. J.
Satoh, Y., see Kigure, T.
Sauder, D. N., see Turnbull, D. H.
Saunders, J.E., see Coleman, A.J.

Scapula
scapula length measurement for assessment of fetal growth and development (Dilmen), 139

Scarring
elasticity imaging for early detection of renal pathology (Emelianov), 871

Scatter
a study of the relationship between mechanical and ultrasonic properties of dystrophic and normal skeletal muscle (Hete), 343
characterization of ultrasonic B-scans using non-Rayleigh statistics (Molthen), 161
effects of endothelin-1 on renal microvasculature measured using quantitative ultrasound (Insana), 1143
fundamental mechanical limitations on the visualization of elasticity contrast in elastography (Ponnekanti), 533
preliminary investigation of ultrasound scattering analysis to identify women at risk for later invasive cancer. I: motivation and experimental technique for characterization of isolated breast tissue lobules (Burke), 295
preliminary investigation of ultrasound scattering analysis to identify women at risk for later invasive cancer. II: extraction of dominant scattering angle-dependent trends from excised breast tissue (Burke), 305
roles of hematocrit and fibrinogen in red cell aggregation determined by ultrasonic scattering properties (Kitamura), 827
the subtleties of ultrasound images of an ensemble of cells: simulation from regular and more random distributions of scatterers (Hunt), 329

Scatterer distribution
the subtleties of ultrasound images of an ensemble of cells: simulation from regular and more random distributions of scatterers (Hunt), 329

Schalken, J. A., see Cornel, E. B.
Scheier, M., see Gehmacher, O.

Schlieren photography
a Schlieren study of the interaction between a lithotripter shock wave and a simulated kidney stone (Carnell), 721

Schmitt, K., see Becker, G.
Schröder, F. H., see Bangma, C. H.
Schwarz, K. Q., Bezante, G. P. and Chen, X.: when can Doppler be used in place of integrated backscatter as a measure of scattered ultrasound intensity?, 231
Scott, M., see Davison, G.

Seborrhoeic keratosis
a 40–100 MHz B-scan ultrasound backscatter microscope for skin imaging (Turnbull), 79

Seçkin, N., see Dilmen, G.

Segmentation
segmentation and analysis of colour Doppler images of tumour vasculature (Bell), 635

Seidel, G., see Kaps, M.
Semple, J. L., see Turnbull, D. H.

Serial assessment
serial assessment of adnexal masses with transvaginal color Doppler sonography (Fleischer), 435

Sertoli cell
the effect of ultrasound exposure *in utero* on the development of the fetal mouse testis: adult consequences (Carnes), 1247

Sex differences
diameter and compliance in the human common carotid artery:—variations with age and sex (Hansen), 1

Shankar, P. M., see Molthen, R. C.

Shear
a noninvasive method to estimate wall shear rate using ultrasound (Brands), 171,
parameter mapping for the detection of disturbed blood flow (Ferrara), 517
ultrasound backscatter at 30 MHz from human blood: influence of rouleau size affected by blood modification and shear rate (van der Heiden), 817

Shear rate dependence
ultrasound backscatter at 30 MHz from human blood: influence of rouleau size affected by blood modification and shear rate (van der Heiden), 817

Sheep
vascular resistance quantification in high flow resistance areas using the Doppler method (Arbeille), 321

Shiba, A., see Naito, J.
Shimura, T., see Naito, J.

Shock waves
a Schlieren study of the interaction between a lithotripter shock wave and a simulated kidney stone (Carnell), 721
acoustic energy determines haemoglobin release from erythrocytes by extracorporeal shock waves *in vitro* (Delius), 707
biological effects of shock waves: *in vivo* effect of high energy pulses on rabbit bone (Delius), 1219
electronic beam steering of shock waves (Cathignol), 365
flow cytometric analysis of cell suspensions exposed to shock waves in the presence of the radical sensitive dye Hydroethidine (Endl), 569
importance of the implosion of ESWL-induced cavitation bubbles (Delacretaz), 97
influence of water temperature on pressure pulses generated by an electromagnetic type lithotripter (Augat), 89
macroscopic ESWL-induced cavitation: *in vitro* studies, 393
physical factors involved in stress-wave-induced cell injury: the effect of stress gradient (Doukas), 961
the effects of successive high-energy shock-wave tumor administration on tumor blood flow (Cornel), 243
the performance of different pressure pulse generators for extracorporeal lithotripsy: a comparison based on commercial lithotripters for kidney stones (Buizza), 259
thresholds for hemorrhages in mouse skin and intestine induced by lithotripter shock waves (Miller), 249

Shung, K. K. and Flenniken, R. R.: time-domain ultrasonic contrast blood flowmetry, 71
Shung, K. K., see Hete, B.
Siddiqi, T. A., O'Brien, W. D. Jr., Meyer, R. A., Sullivan, J. M. and Miodovnik, M.: *in situ* human obstetrical ultrasound exposimetry: estimates of derating factors for each of three different tissue models, 379
Sigel, B., see Kitamura, H.

Signal processing
a noninvasive method to estimate wall shear rate using ultrasound (Brands), 171
adaptive SVD-based AR model order determination for time-frequency analysis of Doppler ultrasound signals (Fort), 793
effects of endothelin-1 on renal microvasculature measured using quantitative ultrasound (Insana), 1143
the effect of echo suppression on the mean velocity estimation range of the RF cross-correlation model estimator (Brands), 945
velocity matched spectrum analysis: a new method for suppressing velocity ambiguity in pulsed-wave Doppler (Torp), 937
volumetric blood flow calculation using a narrow ultrasound beam (Willink), 203
volumetric blood flow measurement by simultaneous Doppler signal and B-mode image processing: a feasibility study (Willink), 481

Siu, A. K. Q., see Burke, T. M.

Skeletal muscle
a study of the relationship between mechanical and ultrasonic properties of dystrophic and normal skeletal muscle (Hete), 343

Skin
a 40–100 MHz B-scan ultrasound backscatter microscope for skin imaging (Turnbull), 79
ultrasonic propagation properties of excised human skin (Moran), 1177

Skin imaging
a 40–100 MHz B-scan ultrasound backscatter microscope for skin imaging (Turnbull), 79

Skovoroda, A. R., see Emelianov, S. Y.
Sladkevicius, P. and Valentin, L.: reproducibility of Doppler measurements of blood flow velocity in the uterine and ovarian arteries in premenopausal women, 313

Small-for-date fetuses
assessment of fetal left cardiac isovolumic relaxation time in appropriate and small-for-gestational-age fetuses (Tsyvian), 739

Smielewski, P., Czosnyka, M., Iyer, V., Piechnik, S., Whitehouse, H. and Pickard, J.: computerised transient hyperaemic response test—a method for the assessment of cerebral autoregulation, 599
Smievoll, A. I., see Gilja, O. H.
Smith, S. W., Lopath, P. D., Adams, D. B. and Walcott, G. P.: cardiac ultrasound phantom using a porcine heart model, 693
Smits, G. A. H. J., see Cornel, E. B.
Sokil-Melgar, J., see Ferrara, K. W.
Sokil-Melgar, J., see Kitamura, H.
Sonesson, B., see Hansen, F.
Spaan, J. A. E., see Bos, L. J.
Spagno, C., see Buizza, A.

Speckle
blood perfusion measurement with multifrequency Doppler ultrasound (Eriksson), 49
discrimination of intravascular lumen and dissections in single intravascular ultrasound images using subtraction, conventional averaging and saline flush (Pasterkamp), 149
registration of three-dimensional compound ultrasound scans of the breast for refraction and motion correction (Moskalik), 769
time-domain ultrasonic contrast blood flowmetry (Shung), 71

Speckle tracking
experimental velocity profiles and volumetric flow via two-dimensional speckle tracking (Bohs), 885
time-domain ultrasonic contrast blood flowmetry (Shung), 71
ultrasound tissue displacement imaging with application to breast cancer (Chen), 1153

Spectral analysis
acoustic energy determines haemoglobin release from erythrocytes by extracorporeal shock waves *in vitro* (Delius), 707
adaptive SVD-based AR model order determination for time-frequency analysis of Doppler ultrasound signals (Fort), 793
demonstration of three-dimensional vector flow estimation using bandwidth and two transducers on a flow phantom (McArdle), 679

roles of hematocrit and fibrinogen in red cell aggregation determined by ultrasonic scattering properties (Kitamura), 827
statistical bias and variance in blood flow estimation by spectral analysis of Doppler signals (Willink), 919
velocity matched spectrum analysis: a new method for suppressing velocity ambiguity in pulsed-wave Doppler (Torp), 937
volumetric blood flow calculation using a narrow ultrasound beam (Willink), 203

Spectral broadening
correction of intrinsic spectral broadening errors in Doppler peak velocity measurements made with phased sector and linear array transducers (Winkler), 1029
Doppler ultrasound spectral shape downstream of significant arterial stenosis *in vivo* (Hutchison), 447

Speed
acoustic properties of some biocompatible polymers at body temperature (Guess), 273
the effect of refraction and assumed speeds of sound in tissue and blood on Doppler ultrasound blood velocity measurements (Christopher), 187
ultrasonic propagation properties of excised human skin (Moran), 1177

Sperm production
the effect of ultrasound exposure *in utero* on the development of the fetal mouse testis: adult consequences (Carnes), 1247

Spontaneous echo contrast
quantification of blood echogenicity: evaluation of a semiquantitative method of grading spontaneous echo contrast (Fatkin), 1191

Stale, H., see Arbeille, P.
Starkoski, B. G., see Turnbull, D. H.
Steinbach, P., see Endl, E.

Stenosis
assessment of regional vascular distensibility in diseased iliofemoral arteries by intravascular ultrasound (The), 17
changes in ultrasonic Doppler backscattered power downstream of concentric and eccentric stenoses under pulsatile flow (Cloutier), 59
Doppler ultrasound spectral shape downstream of significant arterial stenosis *in vivo* (Hutchison), 447
Doppler velocity ratio measurements evaluated in a phantom model of multiple arterial disease (Allard), 471
effects of stenosis on transit-time ultrasound measurements of blood flow (Gordon), 623
parameter mapping for the detection of disturbed blood flow (Ferrara), 517
quantitative investigation of *in vitro* flow using three-dimensional colour Doppler ultrasound (Guo), 807

Stephenson, T. J., see Bird, N. C.

Stochastic processess
statistical bias and variance in blood flow estimation by spectral analysis of Doppler signals (Willink), 919

Stone fragmentation
a Schlieren study of the interaction between a lithotripter shock wave and a simulated kidney stone (Carnell), 721
importance of the implosion of ESWL-induced cavitation bubbles (Delacretaz), 97

Stones
a Schlieren study of the interaction between a lithotripter shock wave and a simulated kidney stone (Carnell), 721
electronic beam steering of shock waves (Cathignol), 365

Strain
elasticity imaging for early detection of renal pathology (Emelianov), 871
fundamental mechanical limitations on the visualization of elasticity contrast in elastography (Ponnekanti), 533

Strangling device
changes in ultrasonic Doppler backscattered power downstream of concentric and eccentric stenoses under pulsatile flow (Cloutier), 59

Streaming
a novel ultrasonic technique for differentiating cysts from solid lesions: preliminary results in the breast (Nightingale), 745
effects of ultrasound on agglutination and aggregation of human erythrocytes *in vitro* (Pohl), 711

Streptokinases
pro- and antifibrinolytic effects of ultrasound on streptokinase-induced thrombolysis (Nilsson), 833

Stress
fundamental mechanical limitations on the visualization of elasticity contrast in elastography (Ponnekanti), 533
physical factors involved in stress-wave-induced cell injury: the effect of stress gradient (Doukas), 961

Stroke
quantification of blood echogenicity: evaluation of a semiquantitative method of grading spontaneous echo contrast (Fatkin), 1191

Sulcova, A., see Hrazdira, I.
Sullivan, J. M., see Siddiqi, T. A.

Surgery
ultrasound focal beam surgery (ter Haar), 1089

Szabo, T. L., see Wu, J.

T

3D Colour Doppler ultrasound
quantitative investigation of *in vitro* flow using three-dimensional colour Doppler ultrasound (Guo), 807

3D Imaging
in vivo comparison of 3D ultrasonography and magnetic resonance imaging in volume estimation of human kidneys (Gilja), 25

intravascular ultrasound image subtraction: a contrast enhancing technique to facilitate automatic three-dimensional visualization of the arterial lumen (Pasterkamp), 913
registration of three-dimensional compound ultrasound scans of the breast for refraction and motion correction (Moskalik), 769
segmentation and analysis of colour Doppler images of tumour vasculature (Bell), 635
ultrasonic three-dimensional reconstruction of the heart (Salustri), 281

3D Reconstruction
in vivo comparison of 3D ultrasonography and magnetic resonance imaging in volume estimation of human kidneys (Gilja), 25
ultrasonic three-dimensional reconstruction of the heart (Salustri), 281

3H-Thymidine incorporation
effect of ultrasound on DNA synthesis in tumor cells (Forytková), 585

Tanaka, S., Kitamra, T., Yoshioka, F., Kitamura, S., Yamamoto, K., Ooura, Y. and Imaoka, T.: effectiveness of galactose-based intravenous contrast medium on color Doppler sonography of deeply located hepatocellular carcinoma, 157
Tapani, E., see Vehmas, T.
Tarantal, A. F., Gargosky, S. E., Ellis, D. S., O'Brien, W. D., Jr. and Hendrickx, A. G.: hematologic and growth-related effects of frequent prenatal ultrasound exposure in the long-tailed macaque (*macaca fascicularis*), 1073

TCD (transcranial Doppler)
is there a hemispheric side preference of cardiac valvular emboli? (Kaps), 753
preoperative and postoperative follow-up in high-grade gliomas: comparison of transcranial color-coded real-time sonography and computed tomography findings (Becker), 1123

Temperature effects
acoustic properties of some biocompatible polymers at body temperature (Guess), 273
damage to red blood cells induced by acoustic cavitation (Daniels), 105
hematologic and growth-related effects of frequent prenatal ultrasound exposure in the long-tailed macaque (macaca fascicularis) (Tarantal), 1073
influence of water temperature on pressure pulses generated by an electromagnetic type lithotripter (Augat), 89
modification of intensity distributions from large aperture ultrasound sources (Clarke), 353
temperature rise generated by diagnostic ultrasound in a transcranial phantom (Wu), 561
ultrasonic heating of the brain of the fetal sheep *in utero* (Duggan), 553
ultrasound focal beam surgery (ter Haar), 1089
ultrasound-guided microwave thermotherapy on a VX-2 carcinoma implanted in rabbit kidney (Kigure), 649

Temperature rise
intestinal hemorrhage from exposure to pulsed ultrasound (Dalecki), 1067
modification of intensity distributions from large aperture ultrasound sources (Clarke), 353

temperature rise generated by diagnostic ultrasound in a transcranial phantom (Wu), 561
ultrasonic heating of the brain of the fetal sheep *in utero* (Duggan), 553
ultrasound focal beam surgery (ter Haar), 1089
ultrasound-guided microwave thermotherapy on a VX-2 carcinoma implanted in rabbit kidney (Kigure), 649

Testicle
ultrasound focal beam surgery (ter Haar), 1089

The, S. H. K., Gussenhoven, E. J., Pieterman, H., van Bortel, L. M. A. B., Li, W., Roelandt, J. R. T. C., de Feyter, P. and van Urk, H.: assessment of regional vascular distensibility in diseased iliofemoral arteries by intravascular ultrasound, 17

Therapy
biological effects of shock waves: *in vivo* effect of high energy pulses on rabbit bone (Delius), 1219
effect of therapeutic ultrasound on endochondral ossification (Wiltink), 121
electronic beam steering of shock waves (Cathignol), 365
flow cytometric analysis of cell suspensions exposed to shock waves in the presence of the radical sensitive dye Hydroethidine (Endl), 569
modification of intensity distributions from large aperture ultrasound sources (Clarke), 353
the effects of successive high-energy shock-wave tumor administration on tumor blood flow (Cornel), 243
ultrasound and microbubbles: their generation, detection and potential utilization in tissue and organ therapy—experimental (Fry), 1227
ultrasound focal beam surgery (ter Haar), 1089
venous thrombosis generation by means of high-intensity focused ultrasound (Delon-Martin), 113

Thermal distribution
ultrasound-guided microwave thermotherapy on a VX-2 carcinoma implanted in rabbit kidney (Kigure), 649

Thermal effects
acoustic properties of some biocompatible polymers at body temperature (Guess), 273
damage to red blood cells induced by acoustic cavitation (Daniels), 105
hematologic and growth-related effects of frequent prenatal ultrasound exposure in the long-tailed macaque (macaca fascicularis) (Tarantal), 1073
influence of water temperature on pressure pulses generated by an electromagnetic type lithotripter (Augat), 89
intestinal hemorrhage from exposure to pulsed ultrasound (Dalecki), 1067
modification of intensity distributions from large aperture ultrasound sources (Clarke), 353
temperature rise generated by diagnostic ultrasound in a transcranial phantom (Wu), 561
ultrasonic heating of the brain of the fetal sheep *in utero* (Duggan), 553
ultrasound focal beam surgery (ter Haar), 1089
ultrasound-guided microwave thermotherapy on a VX-2 carcinoma implanted in rabbit kidney (Kigure), 649

Thermotherapy
ultrasound-guided microwave thermotherapy on a VX-2 carcinoma implanted in rabbit kidney (Kigure), 649

Thomas, R. M., see Miller, D. L.

Thoracic sonography
ultrasound imaging of pneumonia (Gehmacher), 1119

Threshold
histologic effects of high intensity pulsed ultrasound exposure with subharmonic emission in rabbit brain *in vivo* (Vykhodtseva), 969
intestinal hemorrhage from exposure to pulsed ultrasound (Dalecki), 1067
the cavitation threshold of human tissue exposed to 0.2-MHz pulsed ultrasound: preliminary measurements based on a study of clinical lithotripsy (Coleman), 405
thresholds for intestinal hemorrhage in mice exposed to a piezoelectric lithotripter (Dalecki), 1239
ultrasound and microbubbles: their generation, detection and potential utilization in tissue and organ therapy—experimental (Fry), 1227

Thromboembolism
quantification of blood echogenicity: evaluation of a semiquantitative method of grading spontaneous echo contrast (Fatkin), 1191

Thrombolysis
pro- and antifibrinolytic effects of ultrasound on streptokinase-induced thrombolysis (Nilsson), 833
ultrasound accelerates transport of recombinant tissue plasminogen activator into clots (Francis), 419
venous thrombosis generation by means of high-intensity focused ultrasound (Delon-Martin), 113

THRT (transient hyperaemic response test)
computerised transient hyperaemic response test—a method for the assessment of cerebral autoregulation (Smielewski), 599

Thune, N., see Gilja, O. H.

Time domain correlation
volume flow estimation using time domain correlation and ultrasonic flowmetry (Forsberg), 1037

Time series analysis
adaptive SVD-based AR model order determination for time-frequency analysis of Doppler ultrasound signals (Fort), 793

Time-domain flow estimation
time-domain ultrasonic contrast blood flowmetry (Shung), 71

Time-intensity curve
background subtraction from time-intensity curves in videodensitometry: a pitfall in flow assessment using contrast echocardiography (Bos), 1211

Tissue characterization
a study of the relationship between mechanical and ultrasonic properties of dystrophic and normal skeletal muscle (Hete), 343

changes in ultrasonic Doppler backscattered power downstream of concentric and eccentric stenoses under pulsatile flow (Cloutier), 59
characterization of ultrasonic B-scans using non-Rayleigh statistics (Molthen), 161
preliminary investigation of ultrasound scattering analysis to identify women at risk for later invasive cancer. I: motivation and experimental technique for characterization of isolated breast tissue lobules (Burke), 295
preliminary investigation of ultrasound scattering analysis to identify women at risk for later invasive cancer. II: extraction of dominant scattering angle-dependent trends from excised breast tissue (Burke), 305
roles of hematocrit and fibrinogen in red cell aggregation determined by ultrasonic scattering properties (Kitamura), 827
ultrasonic tissue characterization of end-stage dilated cardiomyopathy (Davison), 853
validation of transthoracic myocardial ultrasonic tissue characterization: comparison of transthoracic and open-chest measurements of integrated backscatter (Naito), 33
when can Doppler be used in place of integrated backscatter as a measure of scattered ultrasound intensity? (Schwarz), 231

Tissue displacement
ultrasound tissue displacement imaging with application to breast cancer (Chen), 1153

Tissue heating
modification of intensity distributions from large aperture ultrasound sources (Clarke), 353

Tissue mimic
acoustic energy determines haemoglobin release from erythrocytes by extracorporeal shock waves *in vitro* (Delius), 707

Tissue modelling
in situ human obstetrical ultrasound exposimetry: estimates of derating factors for each of three different tissue models (Siddiqi), 379

Tissue motion
ultrasound tissue displacement imaging with application to breast cancer (Chen), 1153

Tissue perfusion
colour Doppler image analysis for tissue vascularity and perfusion: a preliminary clinical evaluation (Hirsch), 1107
quantification of color Doppler for the evaluation of tissue vascularization (Fein), 1013
ultrasonic estimation of tissue perfusion: a stochastic approach (Adler), 493

Tissue plasminogen activator
ultrasound accelerates transport of recombinant tissue plasminogen activator into clots (Francis), 419

Torp, H. and Kristoffersen, K.: velocity matched spectrum analysis: a new method for suppressing velocity ambiguity in pulsed-wave Doppler, 937
Tortoli, P., Guidi, G. and Newhouse, V. L.: improved blood velocity estimation using the maximum Doppler frequency, 527
Trahey, G. E., see Bohs, L. N.

Trahey, G. E., see Nightingale, K. R.

Trans systolic time
monitoring intracranial dynamics by transcranial Doppler—a new Doppler index: trans systolic time (Hanlo), 613

Transcranial color-coded duplex sonography
preoperative and postoperative follow-up in high-grade gliomas: comparison of transcranial color-coded real-time sonography and computed tomography findings (Becker), 1123

Transcranial Doppler
computerised transient hyperaemic response test—a method for the assessment of cerebral autoregulation (Smielewski), 599
monitoring intracranial dynamics by transcranial Doppler—a new Doppler index: trans systolic time (Hanlo), 613
preoperative and postoperative follow-up in high-grade gliomas: comparison of transcranial color-coded real-time sonography and computed tomography findings (Becker), 1123

Transcranial heating
temperature rise generated by diagnostic ultrasound in a transcranial phantom (Wu), 561

Transesophageal color Doppler
transesophageal color Doppler evaluation of obstructive lesions using the new "Quasar" technology (Fan), 1021

Transesophageal echocardiography
quantification of blood echogenicity: evaluation of a semiquantitative method of grading spontaneous echo contrast (Fatkin), 1191
transesophageal color Doppler evaluation of obstructive lesions using the new "Quasar" technology (Fan), 1021

Transient hyperaemic response
computerised transient hyperaemic response test—a method for the assessment of cerebral autoregulation (Smielewski), 599

Transmitral flow
comparison of diastolic filling models and their fit to transmitral Doppler contours (Nudelman), 989

Transrectal ultrasound
errors in transrectal ultrasonic planimetry of the prostate: computer simulation of volumetric errors applied to a screening population (Bangma), 11
reproducibility and observer variability of transrectal ultrasound measurements of prostatic volume (Collins), 1101
ultrasound focal beam surgery (ter Haar), 1089

Transvaginal color Doppler
serial assessment of adnexal masses with transvaginal color Doppler sonography (Fleischer), 435
the value of transvaginal color Doppler in the assessment of pelvic inflammatory disease (Kupesic), 733

Transverse Doppler
correction of intrinsic spectral broadening errors in Doppler peak velocity measurements made with phased sector and linear array transducers (Winkler), 1029
improved blood velocity estimation using the maximum Doppler frequency (Tortoli), 527
rapid volume flow rate estimation using transverse colour Doppler imaging (Picot), 1199

Triangulation
demonstration of three-dimensional vector flow estimation using bandwidth and two transducers on a flow phantom (McArdle), 679

Tricuspid regurgitation
atrial inflow can alter regurgitant jet size: *in vitro* studies (Grimes), 459

Trophoblasts
glycoprotein and ganglioside changes in human trophoblasts after exposure to pulsed Doppler ultrasound (Heffer-Lauc), 579

Tsyvian, P., Malkin, K. and Wladimiroff, J. W.: assessment of fetal left cardiac isovolumic relaxation time in appropriate and small-for-gestational-age fetuses, 739
Tulleken, C. A. F., see Hanlo, P. W.

Tumour blood flow
effectiveness of galactose-based intravenous contrast medium on color Doppler sonography of deeply located hepatocellular carcinoma (Tanaka), 157
segmentation and analysis of colour Doppler images of tumour vasculature (Bell), 635
the effects of successive high-energy shock-wave tumor administration on tumor blood flow (Cornel), 243

Tumour regression
colour Doppler image analysis for tissue vascularity and perfusion: a preliminary clinical evaluation (Hirsch), 1107
serial assessment of adnexal masses with transvaginal color Doppler sonography (Fleischer), 435

Tumour treatment
echogenicity of experimental liver ethanol injections (Vehmas), 1137
ultrasound focal beam surgery (ter Haar), 1089

Turbulence
changes in ultrasonic Doppler backscattered power downstream of concentric and eccentric stenoses under pulsatile flow (Cloutier), 59
Doppler ultrasound spectral shape downstream of significant arterial stenosis *in vivo* (Hutchison), 447

Turnbull, D. H., Starkoski, B. G., Harasiewicz, K. A., Semple, J. L., From, L., Gupta, A. K., Sauder, D. N. and Foster, F. S.: a 40–100 MHz B-scan ultrasound backscatter microscope for skin imaging, 79
Tysoe, C. and Evans, D. H.: bias in mean frequency estimation of Doppler signals due to wall clutter filters, 671

U

Ueberle, F., see Delius, M.

Ultrasonic echo-tracking
diameter and compliance in the human common carotid artery—variations with age and sex (Hansen), 1

Umbilical artery
umbilical cord venous pulsation in normal fetuses and its incidence after 13 weeks of gestation (Nakai), 443

Umbilical flow
assessment of the fetal PO_2 changes by cerebral and umbilical Doppler on lamb fetuses during acute hypoxia (Arbeille), 861
umbilical cord venous pulsation in normal fetuses and its incidence after 13 weeks of gestation (Nakai), 443

Umbilical vein
umbilical cord venous pulsation in normal fetuses and its incidence after 13 weeks of gestation (Nakai), 443

Unstirred layer
effects of ultrasound on agglutination and aggregation of human erythrocytes *in vitro* (Pohl), 711

van Urk, H., see Pasterkamp, G.
van Urk, H., see The, S. H. K.

Uterine artery
computer analysis of the early diastolic notch in Doppler sonograms of the uterine arteries (Loupas), 1001
reproducibility of Doppler measurements of blood flow velocity in the uterine and ovarian arteries in premenopausal women (Sladkevicius), 313

V

Valentin, L., see Sladkevicius, P.

Valvular emboli
is there a hemispheric side preference of cardiac valvular emboli? (Kaps), 753

Valvular regurgitation
a model based on dimensional analysis for noninvasive quantification of valvular regurgitation under confined and impinging conditions: *in vitro* pulsatile flow validation (Burleson), 899
a numerical and experimental investigation of the flow acceleration region proximal to an orifice (Anayiotos), 501

Valvular stenosis
a numerical and experimental investigation of the flow acceleration region proximal to an orifice (Anayiotos), 501
transesophageal color Doppler evaluation of obstructive lesions using the new "Quasar" technology (Fan), 1021

Vandeursen, H., see Delacrétaz, G.
Vandeursen, H., see Pittomvils, G.

Varicose disease
venous thrombosis generation by means of high-intensity focused ultrasound (Delon-Martin), 113

Vector velocity
experimental velocity profiles and volumetric flow via two-dimensional speckle tracking (Bohs), 885

Vehmas, T. and Tapani, E.: echogenicity of experimental liver ethanol injections, 1137

Velocity
a noninvasive method to estimate wall shear rate using ultrasound (Brands), 171
comparison of diastolic filling models and their fit to transmitral Doppler contours (Nudelman), 989
correction of intrinsic spectral broadening errors in Doppler peak velocity measurements made with phased sector and linear array transducers (Winkler), 1029
demonstration of three-dimensional vector flow estimation using bandwidth and two transducers on a flow phantom (McArdle), 679
effects of nonuniform insonation by catheter-tipped Doppler transducers on velocity estimation (Moraes), 779
experimental velocity profiles and volumetric flow via two-dimensional speckle tracking (Bohs), 885
feasibility study for a two-dimensional diagnostic ultrasound velocity mapping system (Phillips), 217
improved blood velocity estimation using the maximum Doppler frequency (Tortoli), 527
quantitative investigation of *in vitro* flow using three-dimensional colour of Doppler ultrasound (Guo), 807
rapid volume flow rate estimation using transverse colour Doppler imaging (Picot), 1199
reproducibility of Doppler measurements of blood flow velocity in the uterine and ovarian arteries in premenopausal women (Sladkevicius), 313
statistical bias and variance in blood flow estimation by spectral analysis of Doppler signals (Willink), 919
the butterfly search technique for estimation of blood velocity (Alam), 657
time-domain ultrasonic contrast blood flowmetry (Shung), 71
transesophageal color Doppler evaluation of obstructive lesions using the new "Quasar" technology (Fan), 1021
velocity matched spectrum analysis: a new method for suppressing velocity ambiguity in pulsed-wave Doppler (Torp), 937
volumetric blood flow calculation using a narrow ultrasound beam (Willink), 203

Velocity accuracy
quantitative investigation of *in vitro* flow using three-dimensional colour of Doppler ultrasound (Guo), 807

Velocity ambiguity
transesophageal color Doppler evaluation of obstructive lesions using the new "Quasar" technology (Fan), 1021
velocity matched spectrum analysis: a new method for suppressing velocity ambiguity in pulsed-wave Doppler (Torp), 937

Velocity profile
a noninvasive method to estimate wall shear rate using ultrasound (Brands), 171
experimental velocity profiles and volumetric flow via two-dimensional speckle tracking (Bohs), 885
rapid volume flow rate estimation using transverse colour Doppler imaging (Picot), 1199
statistical bias and variance in blood flow estimation by spectral analysis of Doppler signals (Willink), 919
time-domain ultrasonic contrast blood flowmetry (Shung), 71
volumetric blood flow calculation using a narrow ultrasound beam (Willink), 203

Velocity ratio
Doppler velocity ratio measurements evaluated in a phantom model of multiple arterial disease (Allard), 471

Velocity vectors
feasibility study for a two-dimensional diagnostic ultrasound velocity mapping system (Phillips), 217

Venous pulsation
umbilical cord venous pulsation in normal fetuses and its incidence after 13 weeks of gestation (Nakai), 443

Venugopalan, V., see Doukas, A. G.

Vessel diameter
a wall-less vessel phantom for Doppler ultrasound studies (Rickey), 1163

Vessel wall filter
a noninvasive method to estimate wall shear rate using ultrasound (Brands), 171
the effect of echo suppression on the mean velocity estimation range of the RF cross-correlation model estimator (Brands), 945

Videodensitometry
background subtraction from time-intensity curves in videodensitometry: a pitfall in flow assessment using contrast echocardiography (Bos), 1211
quantification of blood echogenicity: evaluation of a semiquantitative method of grading spontaneous echo contrast (Fatkin), 1191

Viscoelasticity
a survey of the acoustic outputs of diagnostic ultrasound equipment in current clinical use (Henderson), 699

Vogt, C., see Delon-Martin, C.

Volume flow
a wall-less vessel phantom for Doppler ultrasound studies (Rickey), 1163
experimental velocity profiles and volumetric flow via two-dimensional speckle tracking (Bohs), 885
rapid volume flow rate estimation using transverse colour Doppler imaging (Picot), 1199

volume flow estimation using time domain correlation and ultrasonic flowmetry (Forsberg), 1037
volumetric blood flow calculation using a narrow ultrasound beam (Willink), 203
volumetric blood flow measurement by simultaneous Doppler signal and B-mode image processing: a feasibility study (Willink), 481

Volume measurement
errors in transrectal ultrasonic planimetry of the prostate: computer simulation of volumetric errors applied to a screening population (Bangma), 11
in vivo comparison of 3D ultrasonography and magnetic resonance imaging in volume estimation of human kidneys (Gilja), 25
reproducibility and observer variability of transrectal ultrasound measurements of prostatic volume (Collins), 1101
ultrasonic three-dimensional reconstruction of the heart (Salustri), 281 (Review)

Volumetric data set
ultrasonic three-dimensional reconstruction of the heart (Salustri), 281 (Review)

VX-2
ultrasound-guided microwave thermotherapy on a VX-2 carcinoma implanted in rabbit kidney (Kigure), 649
Vykhodtseva, N. I., Kynynen, K. and Daminaou, C.: histologic effects of high intensity pulsed ultrasound exposure with subharmonic emission in rabbit brain *in vivo*, 969

W

Walcott, G. P., see Smith, S. W.
Walker, P. G., see Grimes, R. Y.
Walker, W. F., see Nightingale, K. R.

Wall clutter filtering
bias in mean frequency estimation of Doppler signals due to wall clutter filters (Tysoe), 671
the effect of echo suppression on the mean velocity estimation range of the RF cross-correlation model estimator (Brands), 945

Wall shear rate
a noninvasive method to estimate wall shear rate using ultrasound (Brands), 171

Wall shear stress
quantitative investigation of *in vitro* flow using three-dimensional colour of Doppler ultrasound (Guo), 807

Wang, J.-P., see Harrison, G. H.
Wang, W.-Q., see Wang, Y.-Y.
Wang, Y.-Y. and Wang, W.-Q.: an estimation method for blood flow velocity profiles in vessels, 725 (Letter)

Waveform shape analysis
assessment of the fetal PO_2 changes by cerebral and umbilical Doppler on lamb fetuses during acute hypoxia (Arbeille), 861
background subtraction from time-intensity curves in videodensitometry: a pitfall in flow assessment using contrast echocardiography (Bos), 1211
computer analysis of the early diastolic notch in Doppler sonograms of the uterine arteries (Loupas), 1001
Doppler ultrasound spectral shape downstream of significant arterial stenosis *in vivo* (Hutchison), 447

Weisser, G., see Fein, M.
Weitzel, W. F., see Emelianov, S. Y.
White, K. S., see Frush, D. P.
Whitehouse, H., see Smielewski, P.
Whittingham, T. A., see Henderson, J.
Whittingham, T. A., see Jago, J. R.
Wickline, S. A., see Davison, G.
Wiggins, R. C., see Emelianov, S. Y.
Wijkstra, H., see Aarnink, R. G.
Willemse, J., see Hanlo, P. W.
Willink, R. and Evans, D. H.: statistical bias and variance in blood flow estimation by spectral analysis of Doppler signals, 919
Willink, R. and Evans, D. H.: volumetric blood flow calculation using a narrow ultrasound beam, 203
Willink, R. and Evans, D. H.: volumetric blood flow measurement by simultaneous Doppler signal and B-mode image processing: a feasibility study, 481
Willson, K., see Henderson, J.
Willson, K., see Jago, J. R.
Wiltink, A., Nijweide, P. J., Oosterbaan, W. A., Hekkenberg, R. T. and Helders, P. J. M.: effect of therapeutic ultrasound on endochondral ossification, 121
Winkler, A. J. and Wu, J.: correction of intrinsic spectral broadening errors in Doppler peak velocity measurements made with phased sector and linear array transducers, 1029
Wladimiroff, J. W., see Tsyvian, P.
Wood, J. G., see Insana, M. F.
Worthington, A. E., see Hunt, J. W.
Woydt, M., see Becker, G.
Wu, J., Cubberley, F., Gormley, G. and Szabo, T. L.: temperature rise generated by diagnostic ultrasound in a transcranial phantom, 561
Wu, J., see Winkler, A.J.
Wu, J., Zhu, Z. and Du, G.: nonlinear behavior of a liquid containing uniform bubbles: comparison between theory and experiments, 545

Y

Yamamoto, K., see Naito, J.
Yamamoto, K., see Tanaka, S.
Yang, S., see Grimes, R. Y.
Yoganathan, A. P., see Burleson, A. C.
Yoganathan, A. P., see Fan, P.
Yoganathan, A. P., see Grimes, R. Y.
Yoshioka, F., see Tanaka, S.

Young's modulus
elasticity imaging for early detection of renal pathology (Emelianov), 871
fundamental mechanical limitations on the visualization of elasticity contrast in elastography (Ponnekanti), 533

Yuri, Y., see Kigure, T.

Z

Zhu, Z., see Wu, J.
Zuna, I., see Fein, M.

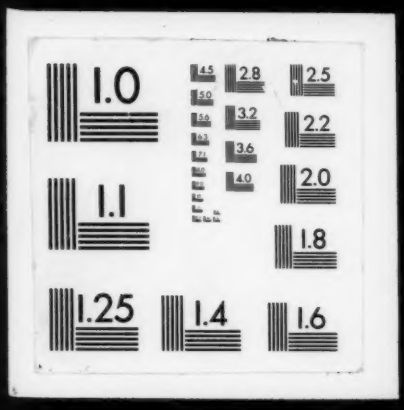
1.0
1.1
1.25
1.4
1.6
1.8
2.0
2.2
2.5
2.8
3.2
3.6
4.0
4.5
5.0
5.6
6.3
7.1
8.0
9.0
10.0